PHILOSOPHICAL TRANSACTIONS OF THE ROYAL SOCIETY A MATHEMATICAL, PHYSICAL & ENGINEERING SCIENCES

Lithospheric Flexure and the Evolution of Sedimentary Basins

A. B. Watts, G. D. Karner and M. S. Steckler

Phil. Trans. R. Soc. Lond. A 1982 **305**, 249-281
doi: 10.1098/rsta.1982.0036

Phil. Trans. R. Soc. Lond. A **305**, 249–281 (1982) [249]
Printed in Great Britain

Lithospheric flexure and the evolution of sedimentary basins†

By A. B. Watts, G. D. Karner and M. S. Steckler
Lamont-Doherty Geological Observatory and Department of Geological Sciences of Columbia University, Palisades, New York 10964, *U.S.A.*

The sediments that have accumulated in sedimentary basins during geological time represent a load on the lithosphere that should respond by flexure. Simple elastic and viscoelastic (Maxwell) plate models have been used to examine quantitatively the contribution of flexure to basin formation. The models have been used to predict the stratigraphy and gravity anomalies associated with basins for different thermal and loading histories. The predictions of the models have been compared with observed stratigraphy and free-air gravity anomalies from interior and cratonic basins. The best overall fit to the observations is for an elastic plate model in which the flexural strength of the lithosphere increases with age. A similar model has recently been used successfully to explain observations from continental margin basins, oceanic islands and seamounts, and deep-sea trench–outer rise systems. This model explains the increase in the overall width of basins during their evolution as well as the stratigraphy of the basin edges. The apparent decrease in the widths of some basins through time can be explained by the model if sediment deposition is followed by erosion of the basin and its edges. The models results suggest that the flexural properties of continental and oceanic lithosphere are generally similar and that flexure is an important factor to consider in backstripping studies in which the tectonic subsidence of a basin is isolated and stratigraphic studies in which relative changes of sea level are estimated.

1. Introduction

Sedimentary basins are dominated during their evolution by epeirogenic or vertical movements of the Earth's crust. Although an individual basin may change its tectonic setting during its evolution, most basins can be classified as occurring in either a rifted or an orogenic setting (Sloss & Speed, 1974; Dickinson & Yarborough 1976; Bally & Snelson 1980). Rifted basins (Bally & Snelson 1980) are associated with divergent plate boundaries where extension is dominant, for example, the U.S. Atlantic margin basins (Baltimore Canyon Trough, South Carolina Trough), which are located on transitional crust between ocean and continent, and possibly the North Sea Basin, which occurs on pre-Mesozoic continental crust. Orogenic basins (Bally & Snelson 1980), on the other hand, are associated with convergent plate boundaries where compression is dominant, for example fore-arc basins (Cook Inlet, Alaska) and foreland basins (Appalachian, Alberta and Ganges).

Most early studies of sedimentary basins were concerned with the role of sediment loading in basin formation (Barrell, 1914; Bowie 1922; Lawson 1938; Walcott 1972). The maximum thickness of sediment that can accumulate in a basin is unlikely on isostatic grounds to exceed about 2.5 times the available water depth. Thus the large thickness of shallow-water sediments observed in some basins cannot be attributed to sediment loading alone, and Bowie (1922, p. 282), for example, recognized that forces other than sediment loading were required.

Recent studies have attempted to isolate the effects of these forces by correcting observed sediment accumulations for the consequences of sediment loading (Watts & Ryan 1976; Steckler

† Lamont-Doherty Geological Observatory Contribution no. 3265.

& Watts 1978; Keen 1979; Watts & Steckler 1981). That part of the subsidence of a basin not caused by sediment loading can be isolated by 'backstripping' sediment and water loads progressively through time. Backstripping consists of reconstructing the stratigraphy of a basin for different intervals of time and then progressively unloading the sediments through time. The resulting 'tectonic subsidence' of a basin can then be directly compared with subsidence curves calculated from different geophysical models.

There is now general agreement that the main cause of the tectonic subsidence of basins is thermal contraction after heating of the lithosphere at the time of basin initiation (Sleep 1971; Falvey 1974; Sleep & Snell 1976; Haxby *et al.* 1976; McKenzie 1978; Middleton 1980; Sleep *et al.* 1980). Sleep (1971) and Sleep & Snell (1976) showed that the tectonic subsidence in deep wells in the Michigan and Illinois basins and the U.S. Atlantic continental margin decreased exponentially with time in a manner similar to a mid-ocean ridge. Sleep (1971) proposed that the tectonic subsidence of continental margin basins was caused by crustal thinning after uplift and erosion at the time of continental rifting. There is, however, generally little evidence of extensive erosion at the time of basin initiation, either at continental margins (Kent 1976) or at interior and cratonic basins (Sleep *et al.* 1980); other processes must therefore have caused the crustal thinning in these basins. McKenzie (1978) proposed a model that addressed this problem in which the lithosphere undergoes extension at the time of rifting. The extension causes thinning of the crust and heating of the lithosphere, which subsequently subsides with time. Sclater & Christie (1980) and Sclater *et al.* (1981*a*) have shown that the tectonic subsidence of the North Sea and Pannonian basins can be explained by this model for values of the lithospheric stretching factor, β, in the range 1.5–3.0 (50–200 %).

The determination of the tectonic subsidence of a basin by using backstripping techniques requires, however, detailed information on compaction, palaeobathymetry, sea level, and the lithospheric response to sediment loads for different times during basin evolution. The effects of compaction and palaeobathymetry can usually be estimated from down-hole geological and geophysical well logs (see, for example, Steckler & Watts 1978; Sclater & Christie 1980) and simple models now exist for long-term sea level changes through time (Pitman 1978; Bond 1978; Watts & Steckler 1979). The response of the lithosphere to sediment loads is a more difficult problem. Most backstripping studies have been based on the Airy model of isostasy, in which sediments are locally supported, rather than on the flexure model, in which sediments are supported by the lateral strength of the crust.

Flexure studies in continental and oceanic regions show that in a number of cases the response of the lithosphere to surface loads such as ice sheets, river deltas, and seamounts and oceanic islands can be modelled by a thin elastic or viscoelastic (Maxwell) plate overlying a weak fluid. Those studies that have considered the role of flexure in basin formation (Walcott 1972; Watts & Ryan 1976; Sweeney 1976; Sleep & Snell 1976; Steckler & Watts 1978; Beaumont 1978, 1981; Karner & Watts 1982) are usually based, however, on a preferred model for the lithospheric response to loading. Only Beaumont & Sweeney (1978) have considered the relative importance in basin formation of both elastic and viscoelastic (Maxwell) models.

The purpose of this paper is to examine critically the role of lithospheric flexure in sedimentary basin formation. We shall apply similar sedimentary loads to different mechanical models for the response of the lithosphere. Both elastic and viscoelastic (Maxwell) models will be considered, since these models have been used widely to interpret geological and geophysical observations associated with other types of loads on the Earth's surface. The stratigraphy and gravity anomaly

for basins will be calculated by using different thermal and loading histories, and comparisons will be made with observations to estimate the best-fitting flexural model. We shall then examine the implications of the best-fitting model to studies of the rheology of continental lithosphere, the tectonic subsidence of basins, and variations of sea-level through time.

2. Lithospheric flexure

The principal evidence for a strong lithosphere has come from studies of its responses to surface loads such as ice sheets (Walcott 1970*a*), seamount chains (Walcott 1970*c*; Watts & Cochran 1974; Watts 1978), isolated seamounts and oceanic islands (Watts *et al.* 1975; McNutt & Menard 1978; Cazenave *et al.* 1980), sediments (Walcott 1972; Cochran 1973; Sleep & Snell 1976; Beaumont 1981), an oceanic or continental plate as it approaches a deep-sea trench (Walcott 1970*c*; Hanks 1971; Watts & Talwani 1974; Caldwell *et al.* 1976; Caldwell 1979) and the relation of topography and gravity anomalies in the interiors of continental (McGinnis 1970; Walcott 1970*b*; Banks *et al.* 1977; McNutt & Parker 1978) and oceanic plates (McKenzie & Bowin 1976; Detrick & Watts 1979; McNutt 1979). These studies suggest that the response to long-term geological loads can be satisfactorily modelled as either an elastic or a viscoelastic (Maxwell) plate overlying a weak substratum.

The parameters that characterize the flexure of thin elastic or viscoelastic (Maxwell) plates are the flexural rigidity, D, and the Maxwell relaxation time, τ. The elastic thickness of the plate, T_e, is related to D by

$$D = ET_e^2/12(1-\sigma^2), \tag{1}$$

where E is the Young modulus and σ the Poisson ratio. In the elastic model the elastic thickness T_e determines the amplitude and wavelength of flexure and does not depend on the age of the load. The viscoelastic (Maxwell) model, in contrast, is described by T_0, the initial elastic thickness, and τ, the Maxwell relaxation time. The amplitude and wavelength of flexure in the viscoelastic model varies as a function of the age of the load and is given by T_0 and τ. The elastic model can therefore be considered as a viscoelastic model with $\tau \to \infty$.

The most applicable model for studies of the mechanical properties of the lithosphere is the subject of much debate at present. In general, most evidence for the elastic model has come from studies in the oceans, while most evidence for the viscoelastic (Maxwell) model has come from studies in the continents. The effects of viscoelasticity should be more apparent in the continents since the oceans are characterized by younger loads (less than about 55 Ma old), whereas the continents are characterized by loads as old as several hundreds of megayears. The elastic model, however, has been most successful in explaining a wide range of geological and geophysical observations in the oceans. Since sedimentary basins occur on both continental and oceanic lithosphere, we shall consider both models in this study.

(*a*) *Elastic model*

The results of most recent flexure studies in the oceans are summarized in table 1 and figure 1. Figure 1 shows the estimates of elastic thickness, T_e, plotted as a function of the age of the plate at the time it was loaded. This figure is similar to an earlier plot by Watts *et al.* (1980) but includes one additional estimate. The estimates of T_e in figure 1 are based on different loads on oceanic lithosphere, which include the topographic relief of oceanic layer 2 (solid squares), river deltas (open circles), seamounts and oceanic islands (solid circles), and deep-sea trench–outer rise

systems (solid triangles). The age of the plate at the time of loading was estimated for each load by subtracting the age of the load from the age of the underlying sea floor.

The main result shown in figure 1 is that T_e *increases* with the age of the oceanic lithosphere at the time of loading. Thus loads emplaced on young lithosphere are associated with small values of T_e while loads formed on old lithosphere are associated with large values. Figure 1 shows that there is good general agreement between T_e and the 300–600 °C oceanic isotherms based on the cooling plate model. This result was interpreted by Watts (1978) as indicating that as the oceanic lithosphere increases in age it becomes more rigid in its response to surface loads.

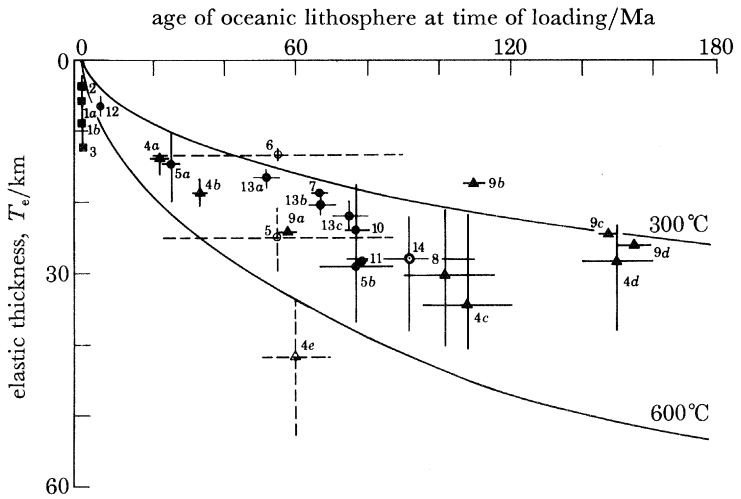

FIGURE 1. Plot of elastic thickness, T_e, against age of the oceanic lithosphere at the time of loading. The sources of the data are summarized in table 1. The broken lines indicate estimates that either represent broad regions rather than an individual geological feature (5, 6) or are considered unreliable (4*e*). The solid lines are the 300 and 600 °C oceanic isotherms based on a cooling plate model.

Figure 1 shows that the estimates of T_e in oceans based on long-term (1–55 Ma) geological loads are one-half to one-third of the seismic thickness based on short-term (*ca.* 150 s) seismic wave periods. Thus on loading there must be rapid relaxation of the oceanic lithosphere from its short-term seismic thickness to its long-term elastic or mechanical thickness. Subsequent relaxation is not observed, but may occur on very long timescales. T_e is therefore acquired soon after loading (less that 1 Ma) and does not appear to change significantly with time.

The results of flexure studies in the oceans are generally compatible with inferences of the rheology of oceanic lithosphere based on data from experimental rock mechanics (Goetze & Evans 1979; Bodine *et al.* 1981). Goetze & Evans (1979) developed a yield stress envelope based on the rheology of olivine in which the yield stress increases, then decreases, with depth. They showed that the oceanic lithosphere could be characterized by an upper part in which deformation occurs by cataclastic flow, and a lower part in which deformation occurs by ductile flow. Between these two regions is a central core that bends elastically but does not develop any permanent deformation. The yield stress model successfully predicts the flexural response for different age oceanic lithosphere while predicting reasonable values for the stresses developed during loading (Bodine *et al.* 1981). The deflexions produced by the yield stress model are in close agreement with those produced by the simple elastic model.

Flexure studies in the oceans are therefore in general support of an elastic plate model for the lithosphere. It is important to point out, however, that the model is referred to as an 'elastic'

Table 1. Summary of oceanic flexure studies

geological feature	age of load t_l / Ma B.P.	age of underlying sea-floor t_{sf} / Ma B.P.	age of sea-floor at time of loading $(t_{sf} - t_l)$ / Ma	effective flexural rigidity, D / 10^{21} Nm	effective elastic thickness, T_e/km ($E = 10^{11}$ Pa, $\sigma = 0.25$)	symbol in figure 1	reference
East Pacific Rise Crest	0	0	0	0.07–20	2–6	1*a*	Cochran (1979)
Juan de Fuca Ridge Crest	0	0	0	4.9	3.8	2	McNutt (1980)
Mid-Atlantic Ridge Crest	0	0	0	3–19	7–13	1*b*	Cochran (1979)
Mid Atlantic Ridge Crest	0	0	0	16	12.2	3	McKenzie & Bowin (1976)
Western Walvis Ridge	*ca.* 5	0	*ca.* 5	1.1–4.5	5–8	12	Detrick & Watts (1979)
Nankai Trough	0	19–25	19–25	19–40	13–16.5	4*a*	Caldwell (1979)
Emperor Seamounts north of 40° N	52–58.5	80†	22.5–28	10–71	10.5–20.0	5*a*	Watts (1978)
Middle America Trench	0	30–35	30–35	40–80	16.5–20.8	4*b*	Caldwell (1979)
Pacific Ocean atolls	0‡	20–90	20–90	17–25	12.4–14.1	6	McNutt & Menard (1978)
Marquesas Island	1–4	*ca.* 44–46	*ca.* 40–45	40	16.5	13*a*	Cazenave *et al.* (1980)
Aleutian Trench	0	55–60	55–60	120	24.3	9*a*	Caldwell *et al.* (1976)
Aleutian Trench	0	50–70	50–70	370–1400	24.6–54.6	4*e*	Caldwell (1979)
Great Meteor Seamount	11–16§	80	64–69	60	18.9	7	Watts *et al.* (1975)
Society Islands	0.5–4	*ca.* 70	*ca.* 66–69	80	20.8	13*b*	Cazenave *et al.* (1980)
Hawaiian Ridge south of 40° N	3–48.5	80–115	66.5–87	39–450	17.5–37.0	5*b*	Watts (1978)
Hawaii Island	0–3	80	77–80	200	28.2	11	Walcott (1970*c*)
Hawaiian Ridge	0–6	80	74–80	90–200	20–28.2	10	Suyenaga (1977)
Crozet Island	5	*ca.* 80	*ca.* 75	100	22.5	13*c*	Cazenave *et al.* (1980)
Amazon Cone	*ca.* 20–25‖	100–130	75–110	100–500	22.5–38.4	14	Cochran (1973)
Kuril Trench	0	90–115	90–115	91–590	21.7–40.5	8	McAdoo *et al.* (1978)
Bonin Trench	0	145–150	145–150	120	24.3	9*c*	Caldwell *et al.* (1976)
Mariana Trench	0	150–160	150–160	140	25.1	4*d*	Caldwell *et al.* (1976)
Mariana Trench	0	140–160	140–160	110–140	23.4–38.1	9*d*	Caldwell *et al.* (1976)
Kuril Trench	0	95–120	95–120	91–600	21.7–40.7	4*c*	Caldwell (1979)
Kuril Trench	0	95–120	95–120	50	17.5	9*b*	Caldwell *et al.* (1976)

† Age uncertain. Based on a model in which the Emperor Trough is a fracture zone offset.
‡ Ages may range to about 15 Ma (Jarrard & Turner 1979).
§ Age based on Wendt *et al.* (1976).
‖ Age based on Kumar (1978).

PHILOSOPHICAL TRANSACTIONS OF THE ROYAL SOCIETY A MATHEMATICAL, PHYSICAL & ENGINEERING SCIENCES

plate model even though T_e changes with time. For a single loading event the lithosphere relaxes rapidly from its short-term seismic thickness to an asymptotic value that does not change with time. Subsequent loading events, however, are emplaced on a lithosphere with a greater value of T_e due to its increase in flexural strength with age.

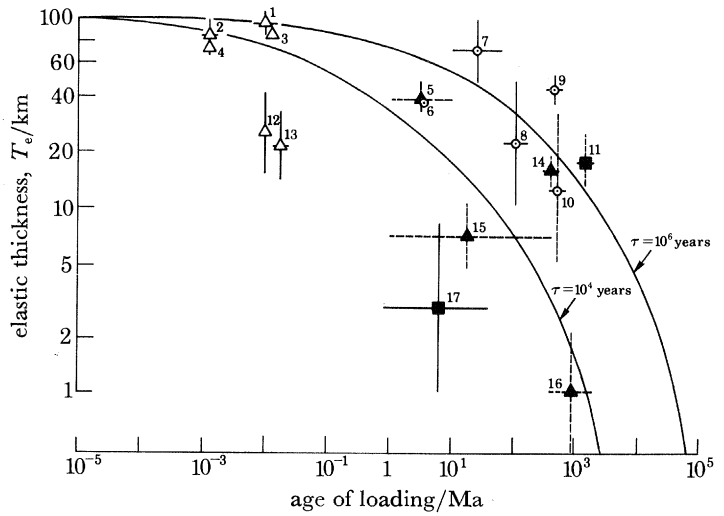

FIGURE 2. Plot of elastic thickness, T_e, of the continental lithosphere against age of load. The sources of data are summarized in table 2. The broken lines indicate estimates in which the age of load is uncertain due either to the broad extent of the region (14–16) or unreliable age data (10–11, 5–6). The solid lines show the calculated T_e based on a viscoelastic (Maxwell) plate with values of the relaxation time $\tau = 10^4$ and 10^6 years.

(*b*) *Viscoelastic (Maxwell) model*

The results of most recent flexure studies in the continents are summarized in table 2 and figure 2. Figure 2 shows the elastic thickness of the continental lithosphere, T_e, plotted as a function of the age of the load. This figure is therefore similar to an earlier plot by Walcott (1970*c*), but differs in including more recent estimates of T_e. The estimates of T_e in figure 2 are based on different loads on the continental lithosphere, including ice sheets (open triangles), sediments (open circles), mountain ranges (solid triangles) and continental rifts (solid squares). The age of the load was estimated from the available geological data. For the East Africa rift system we assumed an age of 0–30 Ma for the load because of the relatively recent uplift of the region. Furthermore, we assumed an age for the large continental regions (such as U.S. and Australia) corresponding to that of the most recent major orogeny (McNutt & Parker 1978), since orogenic regions dominate the continental topography spectra. The age range of loads in figure 2 therefore varies from nearly 0 Ma for East Africa to 1400 Ma for Australia.

The main result shown in figure 2 is that, in contrast to figure 1, T_e appears to *decrease* with age. Thus loads that have been emplaced on the lithosphere for relatively short periods of time are associated with large values of T_e, whereas loads that remain on the lithosphere for longer periods are associated with low values. This suggests that there is a time-dependent stress relaxation that results in a softening of the lithosphere with time. For short times (less than 10^5 years), the elastic thickness of the lithosphere supporting a load is 80–100 km, while for long times (more than 1 Ma), the thickness is much smaller. In the limit ($t \to \infty$), the response approaches that of the Airy model of isostasy.

The data in figure 2 were interpreted by Walcott (1970*c*) as indicating that the lithosphere response to loads as a viscoelastic rather than an elastic plate. The solid lines in figure 2 show the variation of T_e with age that would be expected if the lithosphere responds to loads as a viscoelastic (Maxwell) plate. Figure 2 shows that T_0 in the range 100–110 km and τ in the range 10^4–10^6 years generally constrains the estimates of T_e from the continents. The actual value for τ

TABLE 2. SUMMARY OF CONTINENTAL FLEXURE STUDIES

geological feature	age of load Ma B.P.	basement estimated age Ga B.P.	effective flexural rigidity 10^{21} N m	effective elastic thickness ($E = 10^{11}$ Pa, σ = 0.25)	symbol in figure 2 and figure 16‡	reference
		cratonic setting				
Lake Agassiz	0.007–0.014	1.6–1.8	590–13 200	87–114	1	Walcott (1970*a*)
Lake Algonquin	0.00115–0.00125	1.2–1.5	2900–11 000	69–104	2	Walcott (1970*a*)
Fennoscandia	0.012	2.0–2.8	5900	87	3	McConnell (1968)
Lake Superior	0–0.0012	1.2–1.5	3600	74	4	S. Dutch (unpublished)
Caribou Mountains	1–10?	1.6–1.8?	360–940	34–47	5	Walcott (1970*a*)
Interior Plains	1–10?	1.6–2.5?	598	44	6	Walcott (1970*a*)
Ganges Basin	10–50	1.0–2.0	1000–10 000	48–104	7	Karner (1981)
Odaho/Wyoming Thrust	50–150	0.225–0.325	10–1000	10–48	8	T. E. Jordan (unpublished)
Michigan Basin	370–460	1.2–1.5?	480–1200	38–52	9	Haxby *et al.* (1976)
Boothia Uplift	460–550?	1.6–1.8?	1.2–300	5–32	10	Walcott (1970*b*)
mid-continent gravity high	1100?	1.2–1.5	20–150	13–26	11	McGinniss (1970), Cohen & Meyer (1976)
		orogenic setting				
Lake Hamilton	0.009–0.019	< 0.2	35–600	16–40	12	Fulton & Walcott (1975)
Lake Bonneville	0.015–0.02	< 0.2	24–290	14–32	13	Crittenden (1967, 1970), Walcott (1970*a*)
Northern Great Dividing Range	400–500?	0.4–0.5?	19–60	13–19	14	Wellman (1979)
		uncertain setting				
Continental United States	< 500?	< 0.5?	1.0–10	5–10	15	Banks *et al.* (1977)
Australia	400–1400?	0.4–1.4?	< 0.071	< 2	16	McNutt & Parker (1967)
east Africa	0–30†	0.5–1.4	0.01–50	1–8	17	Banks *et al.* (1977)

† Age of uplift.
‡ Note that only values for which both the age of load *and* basement are considered reliable are plotted in figure 16.

preferred by Walcott (1970*c*) was 10^5 years, which corresponds to an effective viscosity of the lithosphere of 10^{24} P†. Sleep & Snell (1976) and Beaumont (1978, 1981) subsequently used this estimate in their modelling studies of the stratigraphy of the Michigan, North Sea, Canadian foreland and U.S. Atlantic coastal plain basins.

† 1P = 10^{-1} Pa s.

There has been no attempt similar to that of Bodine *et al.* (1981) for the oceans, to establish whether the observations of flexure in the continents are compatible with results from experimental rock mechanics. The main problem is that the continental rheology is too poorly known at present. Thus there is little observational evidence available at present in support of a viscoelastic model for the lithosphere.

3. Simple models of flexure

The stratigraphy of a sedimentary basin is the result of the interaction of a number of different geological processes during time. Backstripping studies have shown that the principal processes affecting the stratigraphy of a basin are thermal contraction and sedimentary loading. Sedimentary factors such as compaction, palaeobathymetry and changes in sea level modify the stratigraphy, but their effects are generally small compared with those of thermal contraction and sedimentary loading. The main problem, therefore in modelling the stratigraphy of basins is determining the form of the thermal contraction and the nature of the basement's response to sediment loads. Thermal contraction controls the overlap shape of the basin that is available for sediments to infill, while the basement response is the main control on the geometry of a basin and the stratigraphy of the basin edges.

We shall first consider the simplest form for the tectonic subsidence of a basin in which the depth available for sedimentation is given by the square root of time since basin initiation. A similar model has been used to describe the subsidence of sea floor less than 70 Ma in age in the oceans (Parsons & Sclater 1977). The shape of the basin is given by

$$Y(x,t) = \begin{cases} 0 & |x| > a, \\ (350/b)\, t^{\frac{1}{2}}(|x| - a) & a \leqslant |x| \leqslant b, \\ 350 t^{\frac{1}{2}} & |x| < b, \end{cases} \tag{2}$$

where t is the time since basin initiation and a and b define the basin width and slope respectively. We assume that sediments infill a broad basin (figure 3) during each $t^{\frac{1}{2}}$ time interval so that the load is constant for any one interval. The sediment load at time t_i is therefore

$$P(x) = (\rho_s - \rho_w)\, g Y_i(x, t_i), \tag{3}$$

where ρ_s is the density of the infilling sediment, ρ_w is the density of the displaced water and g is average gravity.

The form of the tectonic subsidence in figure 3 implies the following sedimentary loading history for a basin:

(1) the basin depth available for sediments decreases with time;

(2) the basin shape is constant during each major depositional cycle (100 Ma);

(3) during each depositional cycle, sediments are transported rapidly from the basin flanks to the basin centre;

(4) peripheral bulges that develop during flexure are eroded to sea level.

The differential equation relating the sedimentary load and basement response for an elastic plate model is given by

$$D\partial^4 y/\partial x^4 + (\rho_m - \rho_{infill})\, g y = P(x), \tag{4}$$

and for a viscoelastic plate model by

$$D\partial^4 \dot{y}/\partial x^4 + (\rho_m - \rho_{infill})\, g[\dot{y} + y/\tau] = P(x)/\tau, \tag{5}$$

where y is the deflexion due to the load $P(x)$, $\dot{y}$ is the first derivative of y with respect to time, ρ_{infill} is the density of the material infilling the deflexion, and ρ_m is the density of the mantle.

The solution to equations (4) and (5) for a load represented in the frequency domain can be expressed as

$$y(k) = \Phi P(k)/(\rho_m - \rho_{infill})\, g, \tag{6}$$

where k = wavenumber and Φ = basement response function. Thus y can be calculated by inverse Fourier transforming (F^{-1}) the product of the response function and the load spectrum.

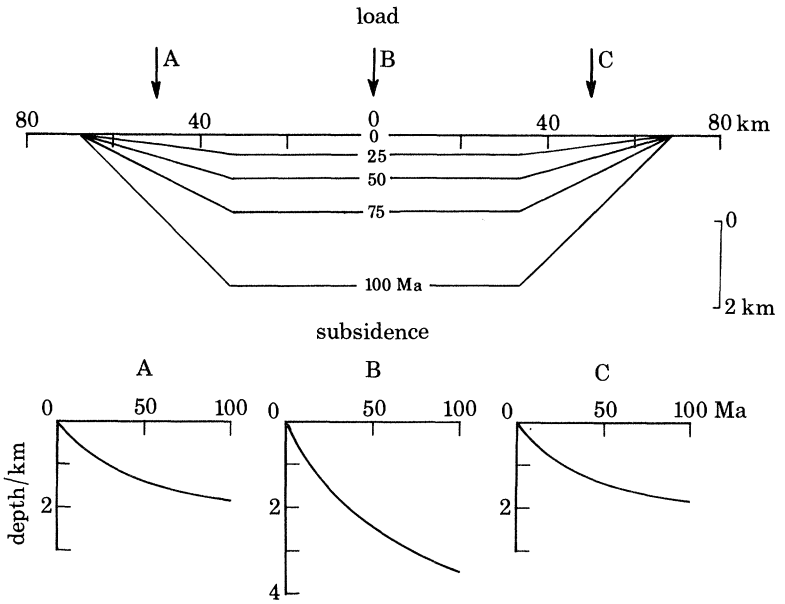

FIGURE 3. Simple model for the tectonic subsidence of a sedimentary basin as a function of age. The subsidence is assumed to decrease exponentially with time, in a manner similar to a mid-ocean ridge. The average width of a basin available for sediments to infill is assumed to remain constant during basin evolution. Vertical exaggeration × 10.

The response functions for both the elastic, $\Phi_e(k)$, and viscoelastic, $\Phi_v(k,t)$, plate models can be obtained (see, for example, Walcott 1976):

$$\Phi_e(k) = 1/(1+C); \tag{7}$$

$$\Phi_v(k,t) = 1 - C\Phi_e(k)\, e^{-t/\tau(1+C)}, \tag{8}$$

where $C = Dk^4/(\rho_m - \rho_{infill})$. For sediments infilling the basin to sea level we then have

$$S_i(x,t_i) = Y_i(x,t_i) + y_i(x,t_i),$$

where $S_i(x,t_i)$ is the sediment accumulation, $y_i(x,t_i)$ is the deflexion, and $Y_i(x,t_i)$ is the tectonic subsidence associated with the ith load and the ith time interval since basin initiation. For an elastic plate we have, for the total sediment thickness,

$$S(x,t_i) = \sum_{i=1}^{N} \left\{ Y_i(x,t_i) + F^{-1}[\Phi_e(k)\, Y_i(k,t_i)] \frac{(\rho_s - \rho_w)}{(\rho_m - \rho_{infill})} \right\}, \tag{9}$$

where $Y_i(k,t_i)$ is the load spectrum, $\Phi_e(k)$ the elastic plate response function for each load increment, and N is the total number of loads. For a viscoelastic plate we have

$$S(x,t_i) = \sum_{i=1}^{N} \left(Y_i(x,t) + F^{-1} \left[\Phi_v(k,t_0)\, Y_i(k,t_i) + \sum_{j=0}^{N-i} \{\Phi_v(k,t_{i+1}) - \Phi_v(k,t_j)\} Y_{i+j}(k,t_{i+j}) \right] \frac{(\rho_s - \rho_w)}{(\rho_m - \rho_{infill})} \right), \tag{10}$$

where t_j and t_{j+1} is the age range of the ith load. Thus $\Phi_e(k)$ and $\Phi_v(k, t)$ must be evaluated for each load applied. For the elastic model, $\Phi_e(k)$ is only evaluated once for each load applied, since once $\Phi_e(k)$ is acquired it does not change subsequently with time. For the viscoelastic model, in contrast, $\Phi_v(k, t)$ has to be evaluated for each load as well as for each underlying load.

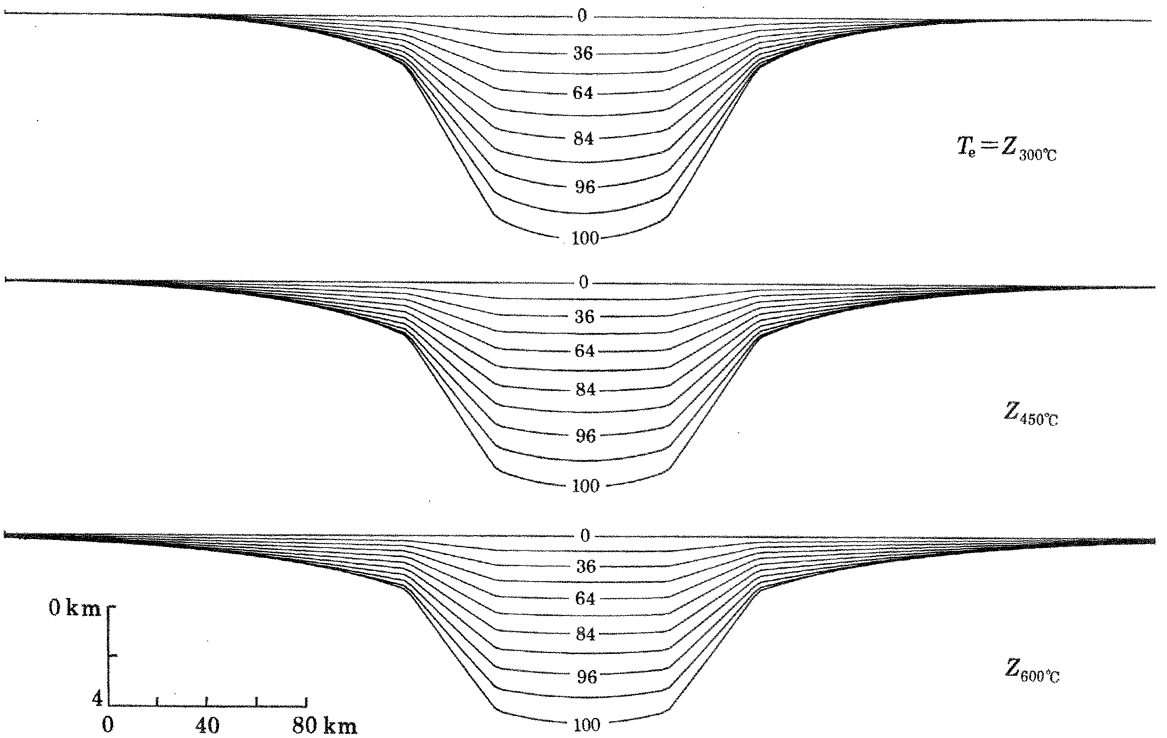

FIGURE 4. Calculated stratigraphy of a sedimentary basin, based on the tectonic subsidence in figure 3 and a simple elastic plate model. The calculations are based on different values of T_e, depending on whether T_e is given by the depth to the 300, 450 or 600 °C oceanic isotherm (figure 1). $T_e = 300$ °C corresponds to the weakest plate and gives the smallest basin width. $T_e = 600$ °C corresponds to the strongest plate and gives the widest basin. All models show a progressive overstepping of younger strata at the margins of the basin, due to the increase of T_e with age. Vertical exaggeration × 10.

The results of the calculations for the stratigraphy of a basin formed on an elastic and viscoelastic plate assuming the load shape in figure 3 are shown in figures 4 and 5. For the elastic model, values of T_e given by the depth to the 300, 450 and 600 °C oceanic isotherms have been used, because these values best describe the flexure observations in figure 1. For the viscoelastic model (figure 5), values of $T_0 = 104$ km ($D_0 = 10^{25}$ N m), and τ of 10^4, 10^5 and 10^6 years have been chosen, because these values apparently best describe the observations in figure 2.

The overall shapes of the basins in figures 4 and 5 are similar for each model. For the elastic models the widths of the basins increase while the amplitudes in the centre decrease as the flexural strength of the basement increases. Similarly for the viscoelastic models, the widths increase while the amplitudes decrease for increasing τ. Both models show a similar overall shape for the most 'rigid' cases with a broad basin overlying a narrow basin.

The elastic and viscoelastic models differ, however, in the stratigraphy predicted at the basin edges. The elastic models (figure 4) show progressive overstepping of younger strata onto basement due to the increase in T_e with age since basin initiation. Sediments that infill the basin soon

after formation load a relatively weak plate, whereas sediments that infill the basin later in its evolution load a relatively strong plate. The viscoelastic models (figure 5), in contrast, show older strata outcropping at the edges of the basin with younger sediments restricted to the basin centre owing to the increasing stress relaxation with age of the load. Thus the youngest sediments in the basin centre show more subsidence and associated peripheral uplift and erosion in flanking regions than the oldest sediments.

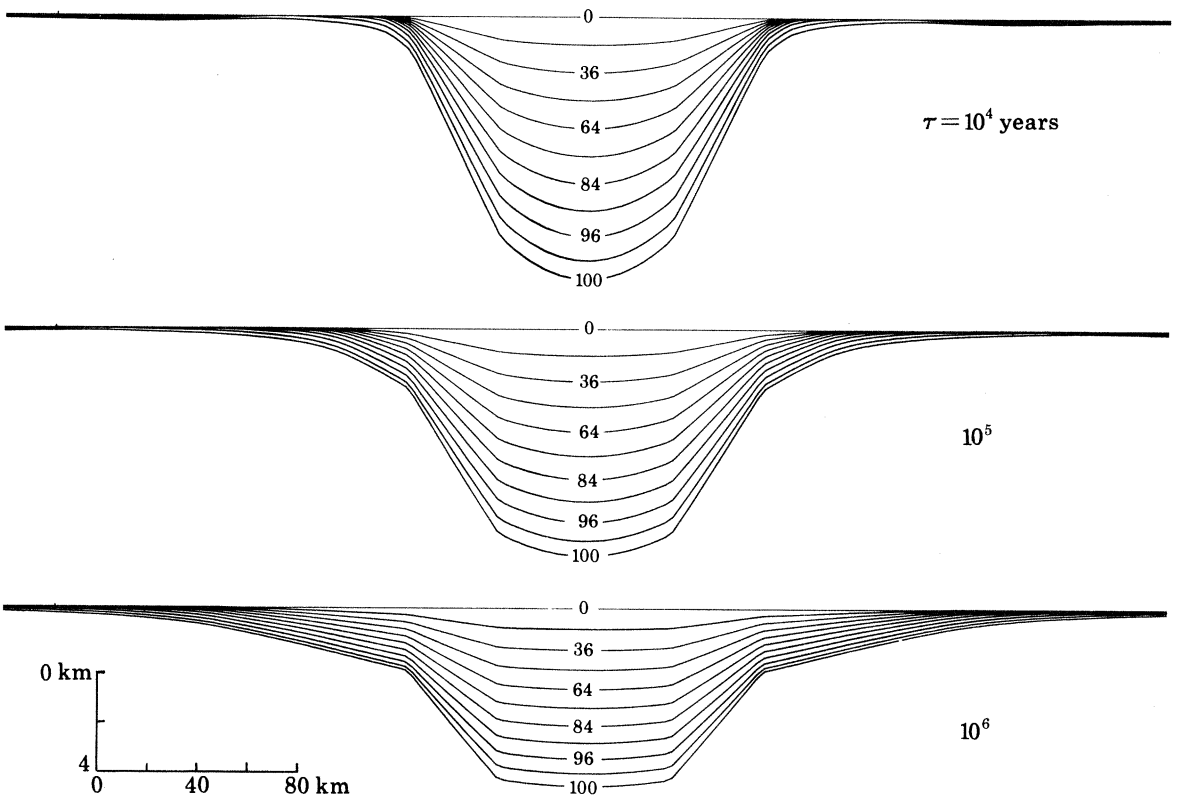

FIGURE 5. Calculated stratigraphy of a sedimentary basin based on the tectonic subsidence in figure 3 and a simple viscoelastic plate model. The calculations are based on different values of τ, in the range 10^4–10^6 years: 10^4 years is associated with the most rapid relaxation and smallest basin width; 10^6 years is associated with the least relaxation and the widest basin. All models show the youngest sediments restricted to the basin centre. Vertical exaggeration $\times 10$.

The direct comparison of the model results to observations is, of course, complicated by the varying ages and geometries of basins that occur in the geological record and the differing effects of sedimentary processes such as compaction, eustasy, transport, and sediment supply in basin formation. The general features of the basin edge stratigraphy can, however, be compared with observations. Figure 6 shows, for example, a stratigraphic cross section of the Gippsland Basin in southeast Australia (Hocking 1976). This basin consists of a late Cretaceous to Eocene formation of terrigeneous sandstones and siltstones overlain either conformably or unconformably by Oligocene to Pliocene marine limestones and calcareous siltstones. The edges of the basin show a progressive onlap of younger sediments onto the basement, similar to the predictions of the elastic model (figure 4). There are a number of other examples in the geological record of basins that show onlap at their edges; the western margin of the West Siberia Basin during the Jurassic and Cretaceous (Zhabrev *et al.* 1975) (figure 6), the coastal plain of northwest Africa (Vail *et al.*

1977), and the North Sea Basin during the Permian (Ziegler 1978). Each example shows a progressive widening of the basin with time after its initiation. Figure 6 shows, in contrast, a stratigraphic cross section of the Michigan Basin in the central U.S. This basin consists of a lower formation of Cambrian–Ordovician sandstones and shales, a middle formation of Silurian–Devonian limestones, dolomites and evaporites, and an upper formation of Carboniferous shales

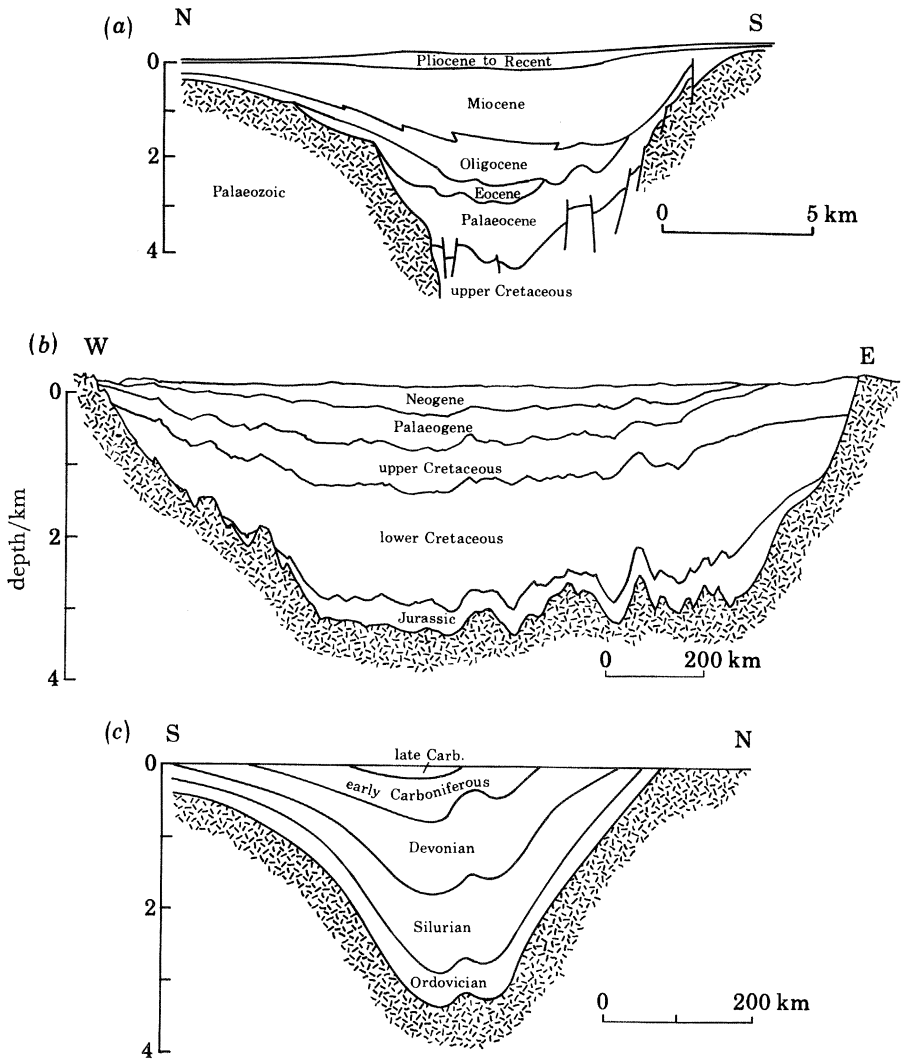

FIGURE 6. Stratigraphic cross section of (*a*) the Gippsland Basin (Hocking, 1976), (*b*) the West Siberia Basin (Zhabrev *et al.* 1975) and (*c*) the Michigan Basin (Sleep & Snell 1976). The Gippsland Basin is an example of a basin that shows progressive onlap of younger sediments on the basement. The Michigan Basin, on the other hand, is an example of a basin in which the younger sediments occur in the centre. The West Siberia Basin shows both types of stratigraphy at its edges. Vertical exaggerations: (*a*) $\times 2$; (*b*) $\times 150$; (*c*) $\times 100$.

and sandstones. The edges of the basin (which are covered in part by a Pleistocene drift) are characterized by younger sediments toward the basin centre, similar to the predictions of the viscoelastic model (figure 5). There are a number of other examples of basins that illustrate this feature; the eastern margin of the West Siberia Basin during the Upper Cretaceous (Zhabrev *et al.* 1975) (figure 6), the North Sea during the late Tertiary (Ziegler & Louwerens 1977), the

Aquitaine Basin during the Neocomian (Winnock 1971), the Paris Basin (B.R.G.M. 1980), and the U.S. Gulf coastal plain (Weaver 1951). Thus both types of model can be recognized in the geological record.

The geometry of stratigraphic horizons in sedimentary basins is determined by the history of subsidence and uplift associated with an individual basin during its evolution. Sloss & Scherer (1975), from a consideration of the geometry of individual stratigraphic horizons, the distance to

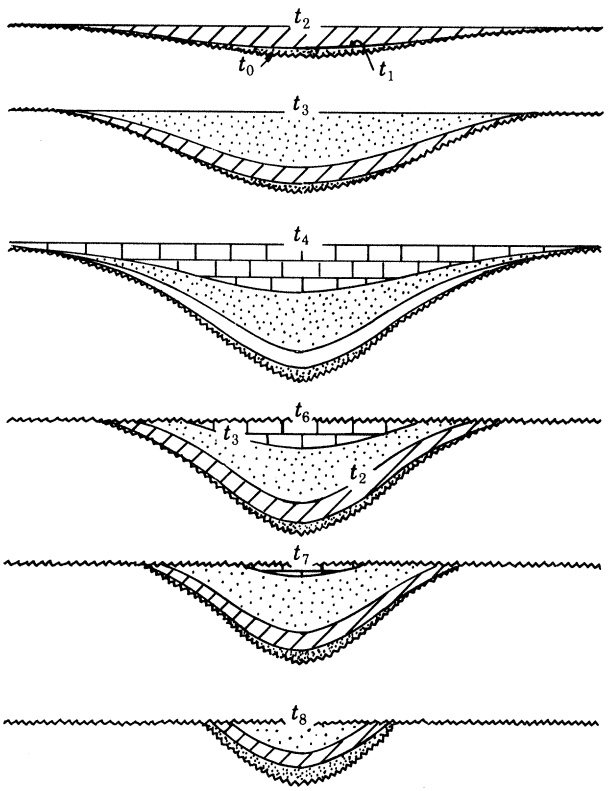

FIGURE 7. Stages in the subsidence, filling and erosion of a sedimentary basin (after Sloss & Scherer 1975).

basin hinge 'lines' (the position of maximum rate of change of sediment thickness), and the thickness of strata, concluded that the Michigan, Williston, and Moscow basins each increased in overall width during their evolution. They proposed a general model for basin evolution in which the basin history changes from an erosional to a depositional cycle and then back to an erosional cycle (figure 7). At time t_0, the depositional cycle is initiated on an essentially planar surface after the completion of a preceding erosional cycle. Deposition between time t_0 and t_1 is confined mainly to the basin centre, but spreads to a greater area between time t_1 and t_2. Differential subsidence continues until time t_4, with subsidence rates decreasing between the basin centre and margins. At time t_4, then, a broad basin exists in which younger sediments progressively onlap basement. After time t_4, the depositional cycle ceases and at some time between t_4 and t_6 the erosional cycle is initiated. By time t_8, a narrow basin exists in which the youngest sediments are restricted to the basin centre.

Figure 7 suggests that an elastic model in which the flexural strength of the lithosphere increases with time could explain configuration of, for example, the Michigan Basin, if the main

deposition cycle in this basin was followed by erosion. Haxby *et al.* (1976), in fact, suggested from detailed stratigraphic studies that T_e increased from the Ordovician to the Devonian in the Michigan Basin. Thus although the present outcrop patterns of the Michigan basin suggest a viscoelastic model, such a model is not required to explain the evolution of this basin.

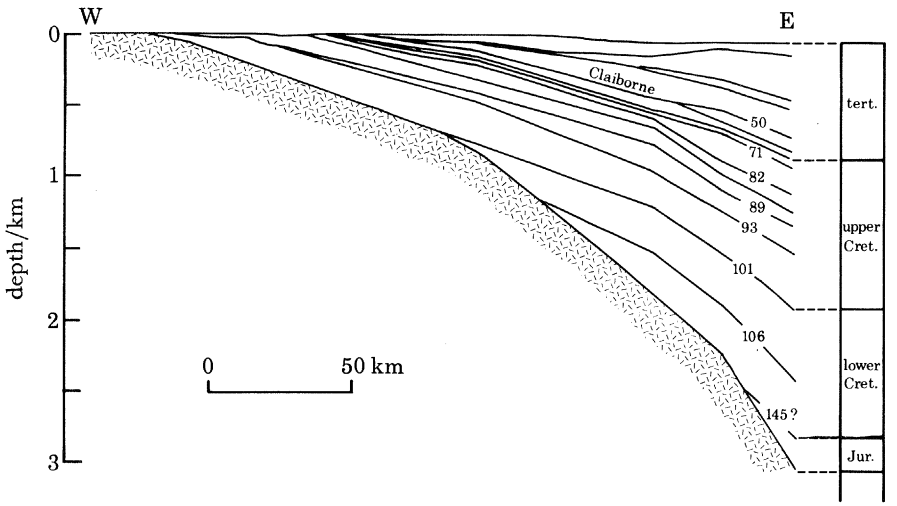

FIGURE 8. Stratigraphic cross section of the U.S. Atlantic coastal plain in North Carolina (after Sleep & Snell 1976). Vertical exaggeration × 50.

A more precise way of estimating whether a basin has been widening during a major depositional cycle is by detailed mapping of marginal sedimentary facies. The problem with basins such as the Michigan, is that much of the facies evidence at the basin edges has been subsequently removed by erosion. Despite their long history, however, the coastal plain of Atlantic-type continental margin basins have not been deeply eroded. Figure 8 shows a geological cross section of the U.S. Atlantic coastal plain in North Carolina, based on well data (Sleep & Snell 1976). The cross section shows progressive onlap of Jurassic to early or late Cretaceous sediments onto Precambrian or Palaeozoic age basement. The late Cretaceous to Tertiary sediments do not onlap basement, and younger sediments progressively subcrop in a seaward direction beneath a Pleistocene cover. Sleep & Snell (1976) interpreted the overall geometry of the coastal plain in terms of a viscoelastic model. Studies of sedimentary facies within the Claiborne (38–49 Ma B.P.), however, show a transgressive sequence of coarse sandstones and silstones of the Conagree formation overlain by fossiliferous highly calcareous limestones of the Santee formation (figure 8) (Colquhoun & Johnson 1968) suggesting the present outcrop pattern of the Claiborne is due to subsequent erosion of the coastal plain (due probably to seaward tilting of the coastal plain). Thus an elastic model in which T_e increases with age followed by erosion could explain the stratigraphy of the U.S. coastal plain.

We have also computed the gravity anomaly predicted by the elastic and viscoelastic models to determine whether observed free-air gravity anomalies can be used to distinguish between these models. The gravity anomaly depends on both the loading history and the basement rheology and so may be a useful model constraint. Figure 9 compares the gravity anomaly predicted by the elastic and viscoelastic models. The calculations assume that the tectonic subsidence of the basin is locally compensated (Airy model), since most thermal models consider basin initiation and rifting to be in local compensation, and that the sediments infilling the

basin load the crust flexurally. Figure 9 shows there is a large spatial variation of the calculated gravity anomalies, which depend on the flexural parameters assumed in the models. The largest amplitude positive anomalies occur over the centre of basins that form on relatively 'rigid' plates ($T_e = Z_{600°C}$; $\tau = 10^6$ years), whereas the largest amplitude negative anomalies occur over the centre of basins that form on relatively weak plates ($\tau = 10^4$ years).

There is a large variation in both amplitude and wavelength of free-air gravity anomalies observed over interior or cratonic basins. For example, the Michigan Basin is associated with generally positive gravity anomalies and the Gippsland Basin is associated with generally

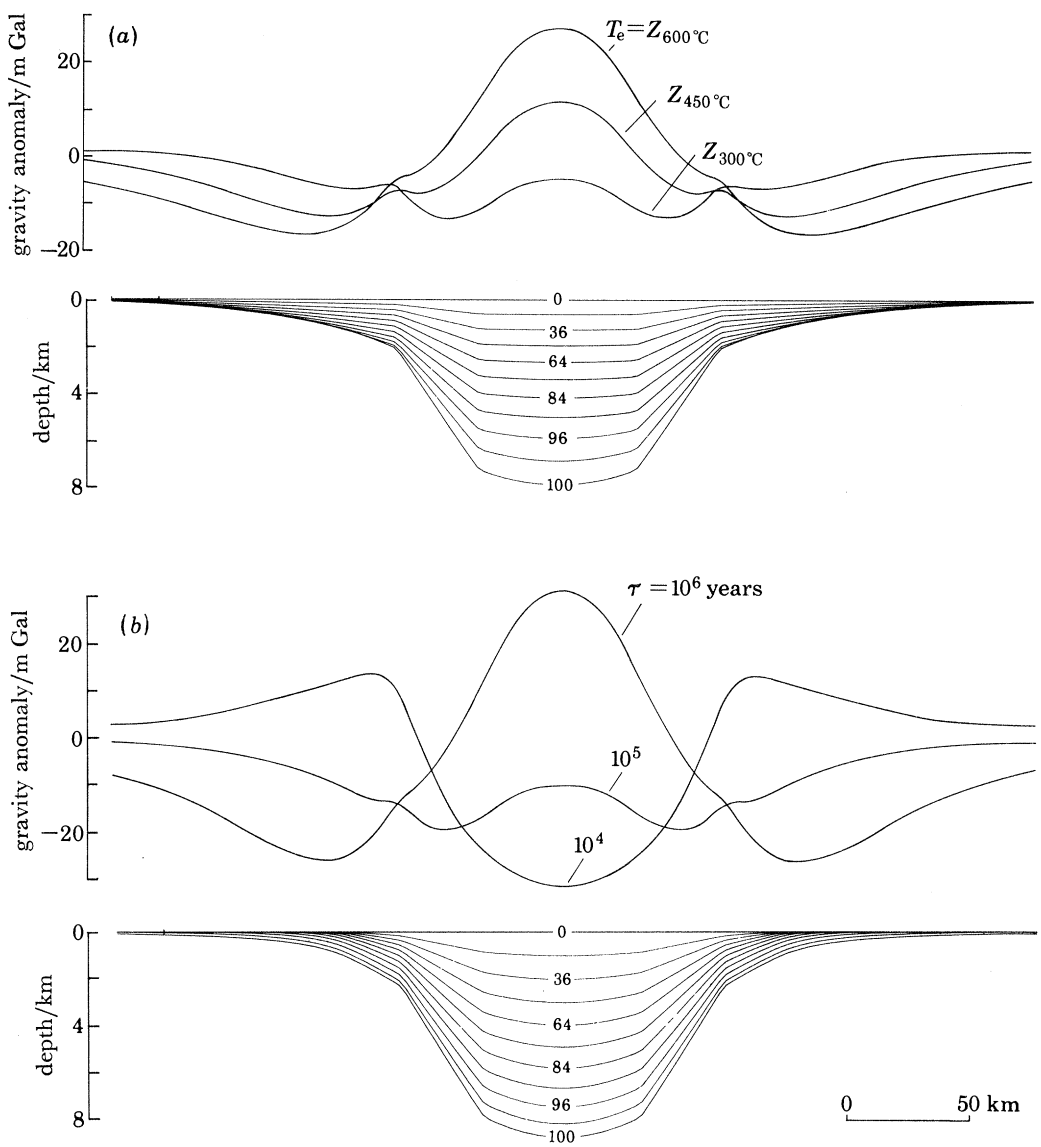

FIGURE 9. Calculated gravity anomalies associated with the sedimentary basins in figures 4 and 5. The upper curves are (*a*) based on the elastic plate model with T_e given by the depth to 300, 450 and 600 °C isotherm, and the lower curves (*b*) are based on the viscoelastic plate model with $T_0 = 104$ km and $\tau = 10^4$, 10^5 and 10^6 years. The tectonic subsidence of the basin is assumed to be due to crustal thinning at the time of basin formation. The crustal thinning has been calculated from the tectonic subsidence assuming Airy isostasy and an initial crustal thickness of 30 km. Vertical exaggeration × 10.

negative anomalies (up to −60 mGal). Furthermore, large-amplitude negative gravity anomalies (up to −60 mGal) characterize basins in the continental shelf north of Scotland (Bott & Watts 1970) and off Nova Scotia (Loncarevic & Ewing 1967), while low-amplitude positive anomalies and nearly zero anomalies characterize the North Sea Basin (Collette 1960), the eastern U.S. continental margin basins (Grow *et al* 1979; Karner & Watts 1982) and major river deltas (Walcott 1972). The model studies suggest that the large variation of observed gravity anomalies over these basins may be due to differences in their tectonic setting on either 'weak' lithosphere (negative anomalies) or 'rigid' lithosphere (positive anomalies), although it is not possible to use the observed gravity anomalies to distinguish between the different flexure models.

4. Thermal and mechanical models

The cooling plate thermal model assumed in the previous section may not be generally applicable to basins because it implies too high temperatures in the lithosphere at the time of their initiation. The basement rocks that have been sampled beneath basins subject to large amounts of subsidence, such as the western Mediterranean (Cravatte *et al.* 1974), the Bay of Biscay (de Charpal *et al.* 1978), and the Michigan Basin (Sleep & Sloss 1978), do not appear to have been extensively reheated.

McKenzie (1978) proposed a thermal model in which the lithosphere undergoes extension at the time of formation of a sedimentary basin. In this model, extension produces thinning and heating of the lithosphere. The amount of extension is defined by a parameter β such that $(1-1/\beta)$ defines the amount of thinning. The model assumes local isostatic equilibrium throughout basin evolution so that there is an initial subsidence due to thinning of the crust followed by a thermal subsidence as heat is conducted to the surface and the lithosphere cools. The case of infinite extension ($\beta \to \infty$), in which the lithosphere is entirely heated, corresponds to the subsidence of a mid-ocean ridge.

The stretching model of McKenzie (1978) has been used to explain the tectonic subsidence of interior basins such as the North Sea Basin (Sclater & Christie 1980; Christie & Sclater 1980; Wood 1981) and the Pannonian Basin (Sclater *et al.* 1981*a*), and continental margin basins such as the western Mediterranean (Steckler & Watts 1980), Bay of Biscay (Le Pichon & Sibuet 1981) and eastern North America (Royden & Keen 1980; Watts 1981). The studies of interior basins suggest β values in the range 1.3–2.0, similar to values inferred for the Basin and Range province of the western U.S. (Proffett 1977), while the studies of continental margin basins show a larger range β ($2 < \beta < 6$). These studies therefore suggest that large amounts of extension (more than 30 %) are associated with the formation of sedimentary basins.

There is now good evidence for faulting and extension during the formation of some interior basins and rifting of continental margin basins. For example, Ziegler (1977) has pointed out two major periods of faulting during the development of the North Sea Basin in Devonian–Carboniferous and Jurassic – early Cretaceous times. Similarly, periods of faulting characterize the development of the continental margins off West Africa, Brazil and northwest Australia (Kent 1976) Jurassic – early Cretaceous in time. Seismic reflexion profiling in basins in the western U.S. (Effimoff & Pinezich 1981) and the Bay of Biscay (de Charpal *et al.* 1978), have shown that the faults are in part listric so that fault movements result in rotation of individual crustal blocks.

PHILOSOPHICAL TRANSACTIONS OF THE ROYAL SOCIETY A MATHEMATICAL, PHYSICAL & ENGINEERING SCIENCES

We have constructed a model in which $Y(x, t)$ in the centre of the basin is given by the stretching model with $\beta = 2.0$ (figure 10). The amount of initial subsidence given by his model, using the parameters in table 3, is 1.73 km and the thermal or tectonic subsidence is given by McKenzie (1978) as

$$Y(x,t) = \begin{cases} 0 & |x| > a \\ (2.095/b)\,(1-\mathrm{e}^{-t/62.8})\,(|x|-a) & a \leqslant |x| \leqslant b \\ 2.095(1-\mathrm{e}^{-t/62.8}) & |x| < b \end{cases} \qquad (11)$$

The depth of the basin is calculated for each $t^{\frac{1}{2}}$ time interval. The shape of the water-filled basin assumed is shown in figure 10 for different times after formation. We used similar assumptions for the loading history of the basin as used in the models in figures 4 and 5.

The results of the calculations for the stratigraphy of a basin based on the stretching model are shown in figure 11 for an elastic and viscoelastic plate. For the elastic model (upper basin) values of T_e are given by the depth to the 450 °C isotherm. For the viscoelastic model, the value of

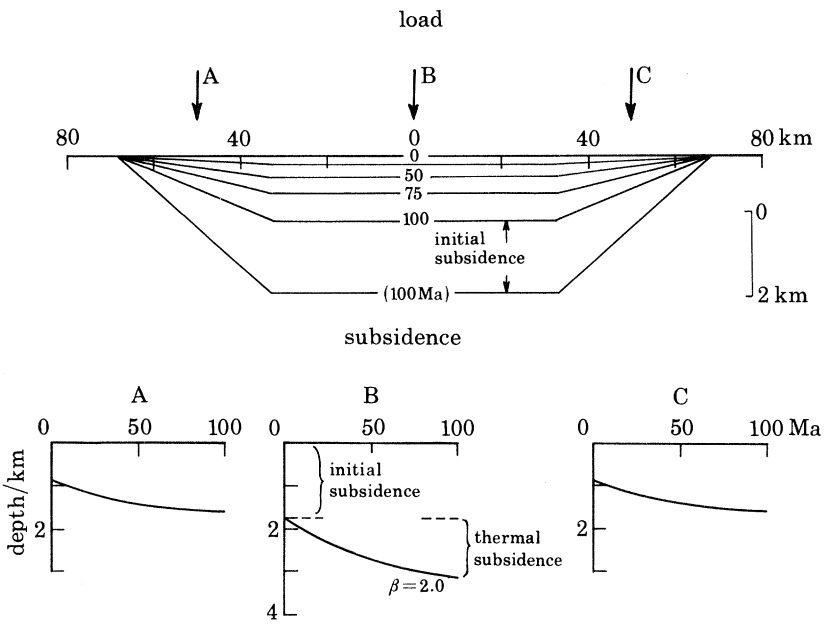

FIGURE 10. Simple model for the tectonic subsidence of a sedimentary basin, based on the stretching model of McKenzie (1978) with $\beta = 2.0$. The subsidence in this model is characterized by an initial subsidence followed by a thermal subsidence that exponentially decreases with time. Vertical exaggeration $\times 10$.

TABLE 3. SUMMARY OF PARAMETERS USED IN MODEL CALCULATIONS

ρ_w	$1.03\ \mathrm{g\ cm^{-3}}$
ρ_s	$2.5\ \mathrm{g\ cm^{-3}}$
ρ_{infill}	$2.5\ \mathrm{g\ cm^{-3}}$
ρ_c	$2.8\ \mathrm{g\ cm^{-3}}$
ρ_m	$3.33\ \mathrm{g\ cm^{-3}}$
E	10^{11} Pa
σ	0.25
L	125 km
T_c	31.2 km
α	$3.4 \times 10^{-5}\ \mathrm{K^{-1}}$
κ	$8.0 \times 10^{-3}\ \mathrm{cm^2\ s^{-1}}$
T_l	1333 °C
g	$981\ \mathrm{cm\ s^{-2}}$

T_0 is given by the depth to the 1109 °C (T_0 = 104 km at $t = \infty$) isotherm and the value of τ is given as 10^5 years. The flexural parameters in both models are obtained by 'tracking' the depths of individual isotherms based on the stretching model. The amplitudes of the basins are similar for each model but the widths are strikingly different. For the elastic model, the sediments that form during the thermal subsidence overstep by about 125 km the sediments that infill the basin formed by the initial subsidence due to the relatively high initial value of T_e and its subsequent increase with age. For the viscoelastic model, in contrast, the magnitude of the overstep is significantly reduced to about 5–10 km owing to the lower initial value of T_0 associated with the heating event and the subsequent increase in stress relaxation with time.

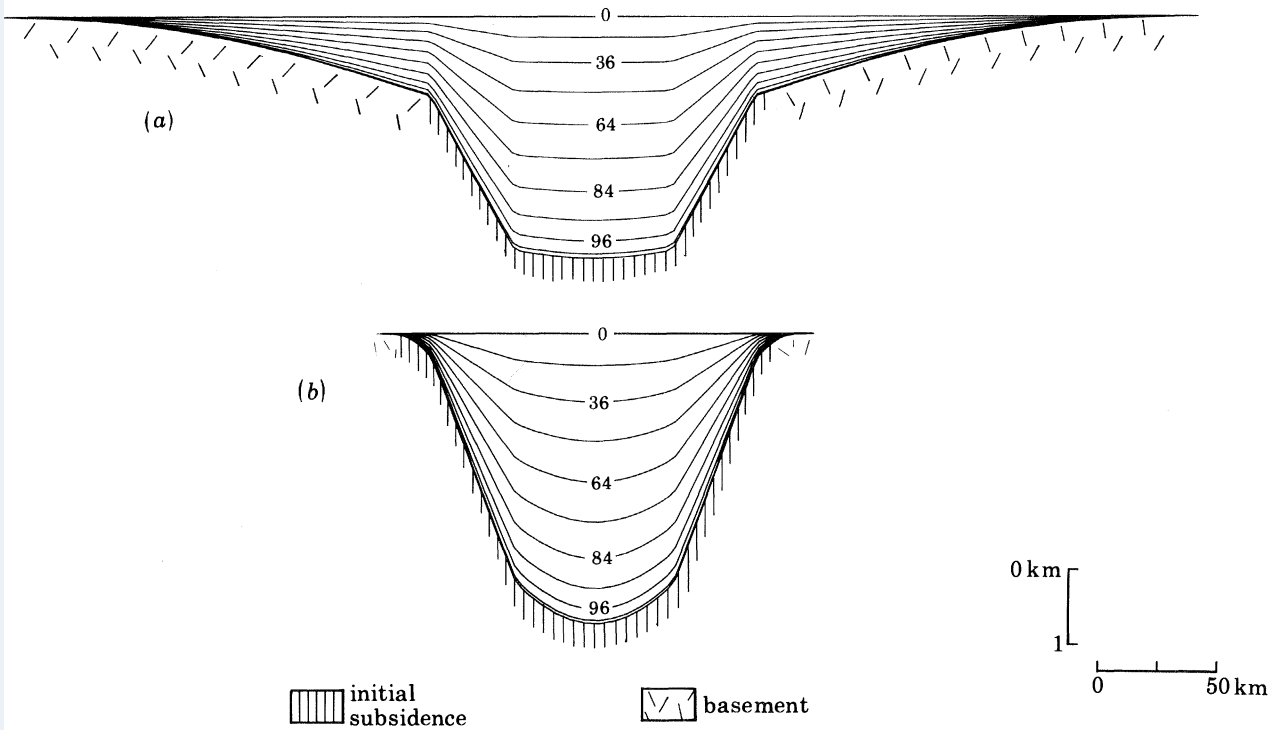

FIGURE 11. Calculated stratigraphy of a sedimentary basin based on the tectonic subsidence in figure 10 and an elastic (*a*) and viscoelastic (*b*) plate model. The elastic model is based on $T_e = Z_{450\,°C}$ and the viscoelastic model is based on $\tau = 10^5$ years and $T_0 = Z_{1109\,°C}$. The sediments that infill the initial subsidence (figure 10) are assumed to load an Airy-type crust, whereas the sediments that infill the thermal subsidence are assumed to load either an elastic plate with T_e increasing with age (*a*) or viscoelastic plate with a constant viscous relaxation time during basin evolution and an initial elastic thickness that increases with age (*b*). Vertical exaggeration × 33.

We have compared the stratigraphy predicted by the elastic and viscoelastic models to interior and cratonic basins that were characterized during their evolution by both fault controlled and thermal or flexural controlled subsidence. Figure 12 shows a stratigraphic cross section of the central North Sea Basin (Ziegler 1977; Ziegler & Louwerens 1977). Rifting was initiated in the basin during the Permian and Trias and continued through the Jurassic and Lower Cretaceous. The greatest subsidence occurred over a relatively narrow region (about 100 km) in the Central graben between the mid-North Sea high and the Stavanger platform. Minor faulting during the Upper Cretaceous was associated with infilling of the earlier graben system, but the Tertiary basin developed as a simple syncline over a broad region. The maximum subsidence occurred

over the region of the fault-controlled central graben. Subsidence extended to flanking regions so that younger Tertiary sediments overstep the older sediment-filled graben by up to 200 km. The overall Late Mesozoic to Tertiary development of the central North Sea Basin therefore generally follows the prediction of the elastic model (figure 11). The main difference with the model is that at the eastern margin of the basin, sediments decrease in age progressively towards the basin centre. The eastern margin appears, however, to have been truncated by late Pleistocene uplift and erosion after ice loading of the Fennoscandian shield (Holtedahl & Bjerkji 1975) so that subsequent sedimentary processes have modified the stratigraphy of one of the edges of this basin.

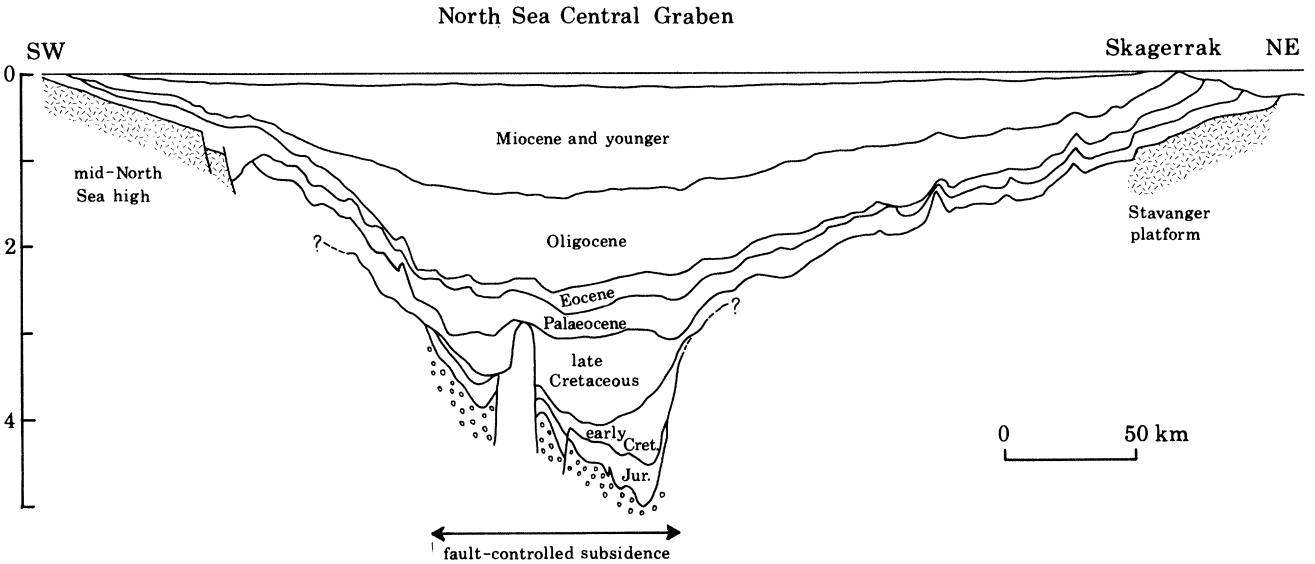

FIGURE 12. Stratigraphic cross section of the North Sea Basin in the region of the Forties and Maureen oil fields, based on Ziegler & Louwerens (1977) and Ziegler (1977). Vertical exaggeration × 33.

There are other examples in the geological record of basins that show a period of fault-controlled subsidence followed by a flexural-controlled subsidence. These include Atlantic-type continental margin basins such as those off eastern North America, Brazil and northwest Australia, and interior or cratonic basins such as the Anadarko, Val Verde, and West Texas in North America (Dewey & Pitman, this symposium) and the Great Artesian Basin in Australia (Tanner 1966). Thus an elastic model in which the basement rigidity increases with time according to the temperature structure defined by the stretching model appears able to explain the overall shape of those basins that were characterized by both oscillatory (Sloss & Speed 1974), or rifting, and submergent, or flexural, depositional cycles. The viscoelastic model, in contrast, does not appear to be able to explain the shape of these basins.

We have not considered in the simple elastic model of figure 11 the effects of lateral variations in the elastic thickness T_e across a basin, or the lateral flow of heat from the stretched region in the centre of the basin to the unstretched basin edges. These effects are difficult to assess because they require a complete knowledge of the thermal structure across a basin. The one-dimensional stretching model can be modified, however, to permit an examination of these effects (see appendix).

The simple elastic model in figure 11 assumes a single constant value for T_e based on the thermal history of the basin centre. In fact, if T_e, corresponds to the depth of the 450 °C isotherm as

suggested by figure 1, then T_e will vary *across* the basin. The centre of the basin will be associated with a value for T_e similar to that assumed in the simple model, but at the edge of the basin, T_e will correspond to that of cold, unstretched lithosphere. In order, therefore, to model correctly the flexure of the lithosphere due to sediment loads, a T_e that varies as a function of time as well as position should be used.

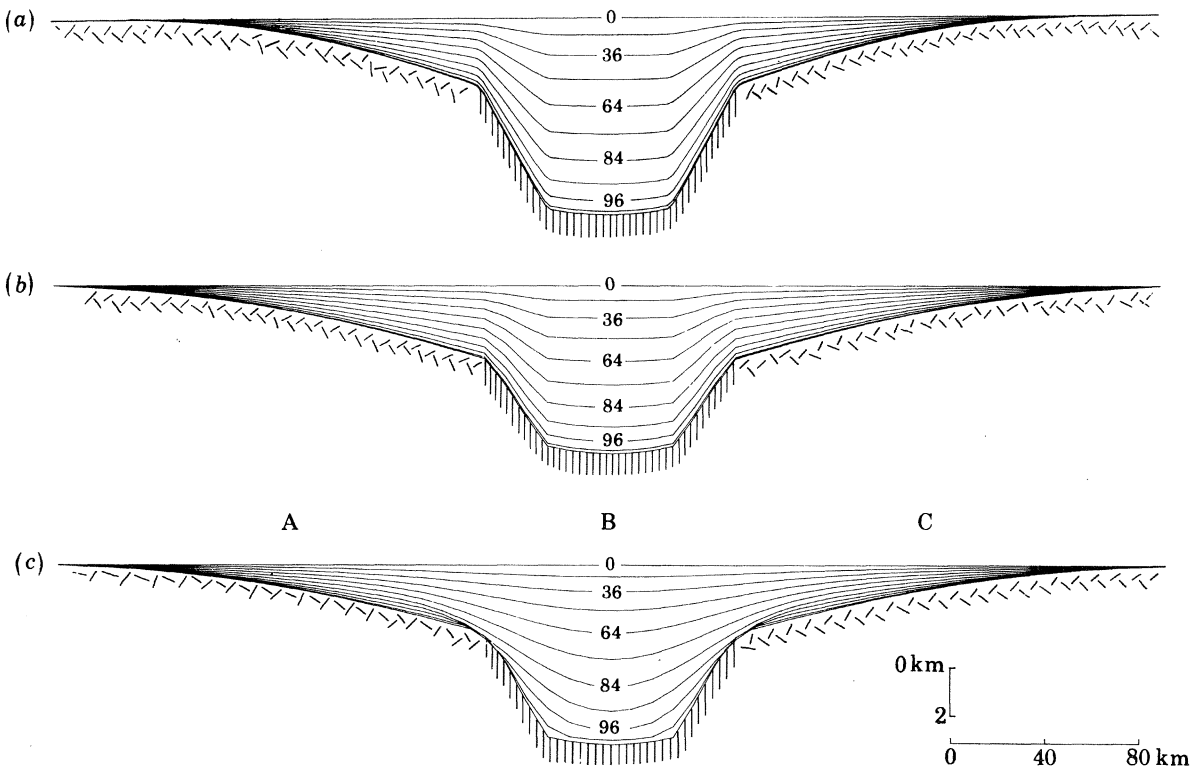

FIGURE 13. Calculated stratigraphy of a sedimentary basin, based on a stretching model with $\beta = 2.0$ (figure 10) and different elastic plate models. (*a*) Flexure is a function of time and T_e is given by the depth to the 450 °C isotherm in the centre of the basin (this model is identical to that in the upper model of figure 11 and is shown for comparison). (*b*) Flexure is a function of time and position and T_e is given by the depth to the 450 °C isotherm across the basin. (*c*) Flexure is a function of time and position, T_e is given by the depth to the 450 °C isotherm across the basin, and the effects of lateral heat conduction are included. Vertical exaggeration $\times 10$.

The appropriate form of the differential equation relating the sediment load and basement response for a variable flexural rigidity is given by

$$\frac{\partial^2}{\partial x^2}\left\{D(x)\frac{\partial^2 y}{\partial x^2}\right\} + (\rho_m - \rho_{infill})\, gy = P(x). \tag{12}$$

This equation can be solved numerically by using a finite difference technique (Bodine 1981). T_e is given by the depth to the 450 °C isotherm at selected points across the basin. By using this technique, the restoring force can also be varied across the basin so that the correct value for $\rho_m - \rho_{air}$ can be used in the region of the flexural bulge.

The stratigraphy of a basin based on a T_e that varies as a function of both time and position across a basin is shown in figure 13*b*. This figure shows that, compared with the simple model of flexure (figure 13*a*), the basin is wider and the progressive onlap of sediments onto the basement

is not as well developed. These features are due to the large T_e associated with the flanks of the basin, which also results in a larger sediment thickness in the flanks relative to the centre of the basin. A greater proportion of the sediments in the centre of the basin occurs early in basin history, when the contrast in T_e across the basin is largest.

The estimate of T_e used to calculate the stratigraphy of the basin in figure 13*b* was based on a model that only considered the vertical cooling of the lithosphere during basin formation. In fact, the heat within the stretched lithosphere will flow laterally as well as vertically, cooling the centre of the basin but heating the unstretched lithosphere of the basin flanks.

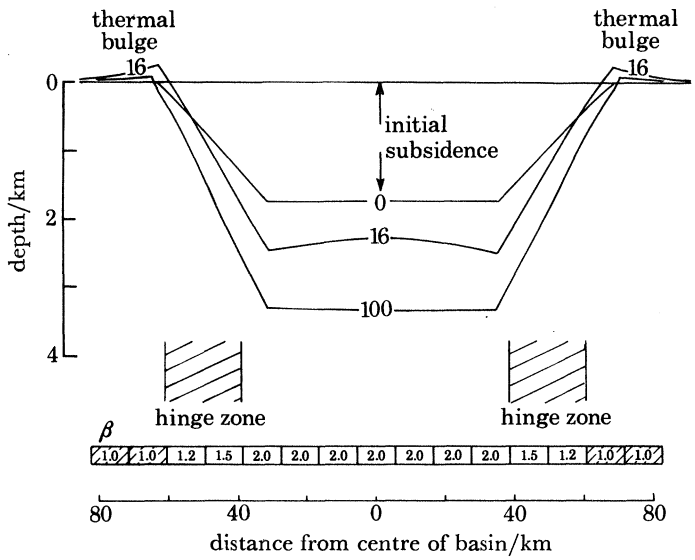

FIGURE 14 Simple model for the variation of the stretching factor β (McKenzie 1978) across a sedimentary basin. The curves show the tectonic subsidence of the basin for 0, 16 and 100 Ma after stretching. The initial subsidence ($t = 0$), which is assumed to occur instantaneously, is similar to the simple model in figure 10. For greater times the lateral flow of heat from the basin produces thermal bulges at the edges of the basin. A corresponding region of increased subsidence occurs in adjoining regions of the basin. Vertical exaggeration $\times 20$.

Figure 14 shows the effects of lateral flow of heat on the overall basin shape. Unlike the simple model in figure 10, the shape of the basin available for sediments does not remain constant during basin evolution. Furthermore, while the initial subsidence is identical, at later times heat flows laterally out of the basin, producing a thermal bulge in flanking regions. The maximum uplift exceeds 250 m and occurs early in the history of the basin. As time progresses, the uplift decreases but also broadens as the heat diffuses outwards. The uplift in the flanks of the basin is accompanied by rapid subsidence on the basin side of the hinge zone. This region loses heat and therefore subsides more rapidly than the centre of the basin. As heat diffuses laterally, the basin flattens out but the position of the basement remains a few hundred metres deeper than the simple model, even after 100 Ma.

We show the effect of including the lateral flow of heat on the stratigraphy of the basin in figure 13*c*. Since heat flows laterally as well as vertically, the lithosphere in the flanking regions is weakened. Thus T_e in flanking regions will decrease so that, compared with figure 13*b*, which only includes flexure varying as a function of time and position, the width of the basin decreases early in its evolution. Near the edge of the unstretched lithosphere, the thermal bulge and

flexure compete, resulting in erosion during the first 16 Ma of basin evolution. In the centre of the basin, the lateral flow of heat results in rapid subsidence and smoothes individual strata. The maximum sediment thickness in figure 13*c* is less than the model in figure 13*a* but a greater proportion of the subsidence occurs early in basin evolution.

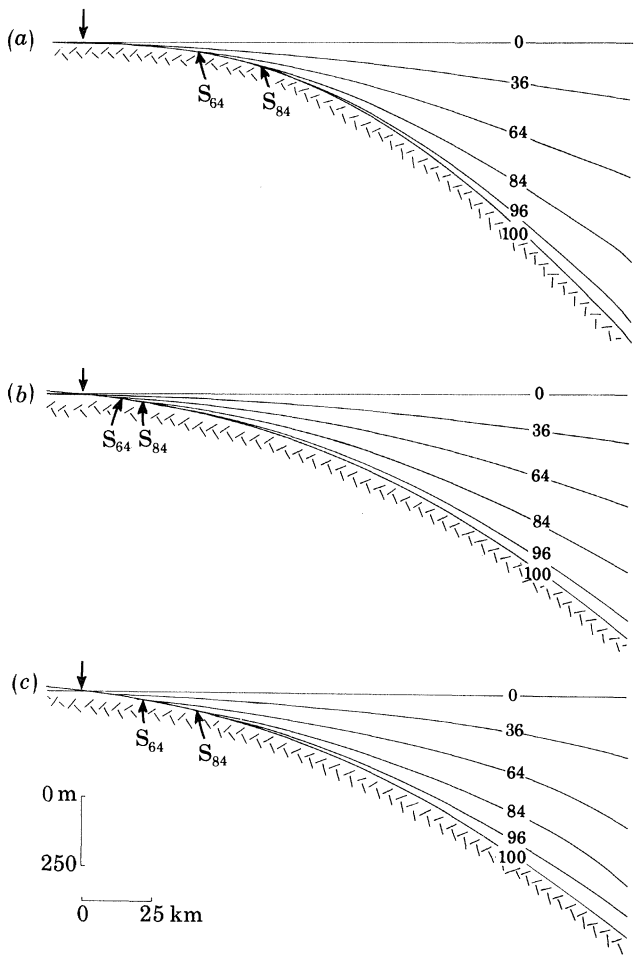

FIGURE 15. Calculated stratigraphy of the edge of the sedimentary basins in figure 14. The heavy sloping arrows indicate the subcrop of the 84 and 64 Ma horizons due to overstepping of younger strata onto the basement. Vertical exaggeration × 100.

Figure 15 shows the details of the stratigraphy at the basin edges for each of the three elastic models. The position of the subcrop of the 64 and 84 Ma horizons and the final stratigraphy at the edge of the basin are shown in the figure. The effect of varying flexure as a function of both time and position (figure 15*b*) causes an increase in the width of the basin and a decrease in the prominence of onlap at the basin edges. The effect of lateral flow of heat (figure 15*c*), however, competes with flexure, causing a decrease in the width and an increase in the prominence of onlap. Thus the stratigraphy of basins that include both the lateral effects of flexure and heat flow (figure 15*c*) closely resembles that of the simple elastic model (figure 15*a*) based only on the one-dimensional heat flow equation.

5. Discussion

We have compared in this study the predictions of simple elastic and viscoelastic (Maxwell) models of loading with observations of the geometry and stratigraphy of sedimentary basins. The best overall fit to these observations is for an elastic model in which the flexural strength of the lithosphere increases with age. We examine in this section the implications of this model to studies of the rheology of continental lithosphere, the tectonic subsidence of basins, and sea level changes through geological time.

(*a*) *Rheology of the continental lithosphere*

The principal evidence for the rheological behaviour of the Earth has come from studies of the manner in which it responds to applied loads. For deformations of the duration of seismic wave periods (a few seconds to a few minutes) the Earth generally behaves as an elastic material. The Earth is not completely elastic at these periods, however, as indicated by finite 'Q' values associated with free oscillation and surface wave data. For deformations of much longer duration (of the order of the age of the Earth) large spatial wavelengths are fully relaxed so that the Earth deforms essentially as a fluid. The duration of loads associated with ice sheets and geological processes (a few thousand to several hundred megayears) is intermediate between those of seismology and the age of the Earth.

A rheology that has been widely used in glacial loading studies is that of a linear viscoelastic (Maxwell) solid. This approximation appears satisfactory because for load durations shorter than the Maxwell relaxation time the response is essentially elastic, while for longer times it becomes viscous. This model can therefore be used to explain both the seismic phenomena at short durations and viscous phenomena at longer durations.

Early studies (for example McConnell 1968) suggested, however, that in order to explain the spectral characteristics of post-glacial rebound some rheological stratification for the Earth was necessary. McConnell (1968) and Peltier (1980) considered models in which there was an upper layer that behaves elastically for the duration of loading overlying a layer of relatively low viscosity. The contribution from an upper elastic layer depends on the spatial wavelength of the applied load (see, for example, Peltier 1980). For relatively long wavelengths the relaxation time is dominated by the viscous properties of the relatively low viscosity layers. For relatively short wavelengths, however, the elastic layer suppresses the viscous response so that the load is completely supported by the upper layer.

The study of loads of small spatial wavelengths provide the best evidence for the long-term mechanical properties of the upper layers of the Earth. Because of the dependence on k^4 in the flexural models, there is a sharp cutoff between short-wavelength loads that are supported by the upper layer and longer-wavelength loads that are comparatively unaffected by the layer.

Walcott (1970*c*) studied the response of the lithosphere to geological loads longer in duration than the Pleistocene ice sheets and concluded that the lithosphere was viscoelastic rather than elastic on long time-scales (1–1000 Ma). He inferred that the lithosphere had a relaxation time in the range 10^4–10^6 years (figure 2). This rheology is consistent with the glacial loading models because for times less than the relaxation time the lithosphere would behave elastically.

We have shown in this study, however, that the overall shape and stratigraphy of sedimentary basins, which represent geological loads of 1–100 Ma on the continental lithosphere, can be satisfactorily explained by an elastic rather than a viscoelastic model. This conclusion is therefore

in contradiction to the results of Walcott (1970*c*). Walcott (1970*c*) noted, however, that a viscoelastic model could not explain the anomalous flexural rigidity associated with Lake Bonneville. This load, which lasted about 10^4 years, is more characteristic of flexural rigidities associated with loads as old as 1 Ma (figure 2). Walcott (1970*c*) suggested that the 'anomalous' Lake Bonneville value could be due to its location within the Basin and Range province of the western U.S., which is characterized by high heat flow, active volcanism and shallow zones with low shear wave velocities.

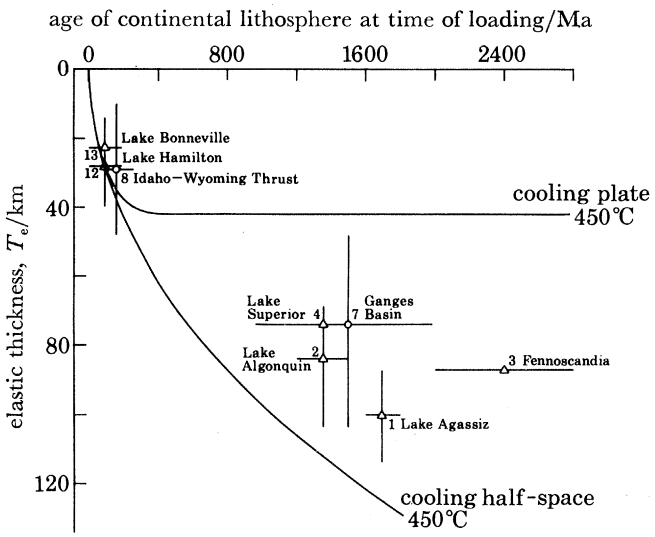

FIGURE 16. Plot of elastic thickness, T_e against age of the continental lithosphere at the time of loading. The sources of the data are summarized in table 2. Estimates 5–6, 10–11 and 14–16 have not been plotted because the age of the load is uncertain, and estimate 9 has not been plotted because the effective age of the basement is uncertain. The solid lines show for comparison the depth to the 450 °C oceanic isotherm based on a cooling plate (upper curve) and cooling half-space model (lower curve).

The low Lake Bonneville value suggests that the flexural rigidity from continents may be influenced by local variations in the thermal structure of continental lithosphere. We therefore need to consider the rigidity of the basement *at* the time of loading. Usually this is obtained by subtracting the age of the load from the age of the basement. However, subsequent thermal events, such as orogeny, basin evolution and heating associated with hot spots, may reset the basement rigidity of continents.

We have examined this possibility by plotting estimates of T_e from the continents against the estimated age of the continental lithosphere at the time of loading (figure 16). We have plotted in figure 16 only those estimates for which both the age of the load and the underlying basement are known (table 2). For example, in the Idaho–Wyoming thrust the age of the load is latest Jurassic to early Eocene (50–150 Ma) and the reset age of the underlying basement is Mississippian to Permian (225–325 Ma) (Jordan 1982). Thus the age of the continental lithosphere at the time of loading for this feature is 75–275 Ma. Furthermore, since the Pleistocene ice sheets are of relatively short duration, the age of the continental lithosphere at the time of loading for these loads is given approximately by the age of the underlying basement.

The main result shown in figure 16 is that there is an apparent increase in T_e from the relatively small values associated with thermally reset continental regions to higher values associated with the more stable interiors of the craton. The solid lines in figure 16 represent the 450 °C

isotherms, based on the cooling plate and half space models, and are shown for comparison with figure 1. Comparison of figures 1 and 16 therefore suggests that T_e for the continental lithosphere increases with age in a manner similar to T_e for the oceanic lithosphere. The small values of T_e in figure 16 can be attributed to the relatively weak, hot lithosphere associated with a thermal event, while the high values of T_e can be attributed to the relatively strong, cold lithosphere associated with the stable craton.

These inferences for the thermal structure of continental lithosphere are in general agreement with the study by Sclater *et al.* (1981 *b*) based on reduced heat flow estimates in the continents. They concluded that in order to explain reduced heat flow values in the continents the thermal perturbations associated, for example, with orogeny should decay at a rate similar to that of the oceans. They concluded that with small modifications the cooling plate model can, in fact, be used to predict the thermal structure of the continents.

The plot in figure 16 therefore suggests that, as well as its response to sediment loading, the mechanical behaviour of continental lithosphere may be generally similar to that of oceanic lithosphere. In addition, an elastic plate model in which T_e increases with age after a thermal event helps to explain the existance of large-amplitude long-wavelength gravity anomalies in stable Precambrian and Palaeozoic terrains, as well as the contrasts in structural styles along some orogenic belts (see, for example, Molnar & Tapponnier 1980). Further work, however, is required to determine whether these inferences of the rheology of continental lithosphere are compatible with data based on experimental rock mechanics.

(*b*) *Tectonic subsidence of sedimentary basins*

We have shown in this study that flexure is an important factor to consider in the development of a sedimentary basin. The role of flexure during basin evolution is controlled by the thermal structure of the basin and varies both as a function of time and position. For example, the cooling plate model predicts that T_e increases from near zero soon after basin formation to 30 km at 100 Ma, whereas the stretching model with $\beta = 2.0$ predicts that T_e increases from about 23 km soon after basin formation to 37 km at 100 Ma. The differences between the models arise because, in contrast to the cooling plate model, the upper lithosphere is not as extensively heated at the time of basin formation in the stretching model.

Flexure should therefore be taken into account in backstripping studies that attempt to isolate the tectonic subsidence of a sedimentary basin. For example, figure 17 shows the total sediment accumulation in the centre of the model basin (figure 13*c*) in which the lithosphere increases its flexural strength with time. The broken line shows the tectonic subsidence that would have been calculated if these sediments were unloaded by using an Airy rather than a flexure model. The solid line for $\beta = 2.0$ represents the tectonic subsidence actually assumed in the calculations. Because the Airy model neglects the effect of the lateral strength of the lithosphere, the difference between the assumed and calculated tectonic subsidence is large (figure 17). In fact, if an Airy model had been used, a best fitting $\beta = 1.6$ would have been estimated, which is significantly smaller than the $\beta = 2.0$ assumed in the calculations. The corresponding amount of extension inferred in the centre of the basin would therefore have been underestimated by about 40 %.

Sclater & Christie (1980) have estimated the amount of stretching in the North Sea Basin by using the tectonic subsidence calculated at selected wells. Although they reconstructed the stratigraphy of the basin at the wells taking into account the effects of compaction and palaeobathymetry, they backstripped the sediments by using an Airy rather than a flexure model. We

PHILOSOPHICAL TRANSACTIONS OF THE ROYAL SOCIETY A MATHEMATICAL, PHYSICAL & ENGINEERING SCIENCES

suggest that flexure is important, even for the relatively wide North Sea Basin, and that the β values obtained by Sclater & Christie (1980) may have been significantly underestimated.

Clearly, additional data, such as fault geometry and seismic reflexion and refraction data, are required to better constrain stretching estimates of sedimentary basins that are based only on well data.

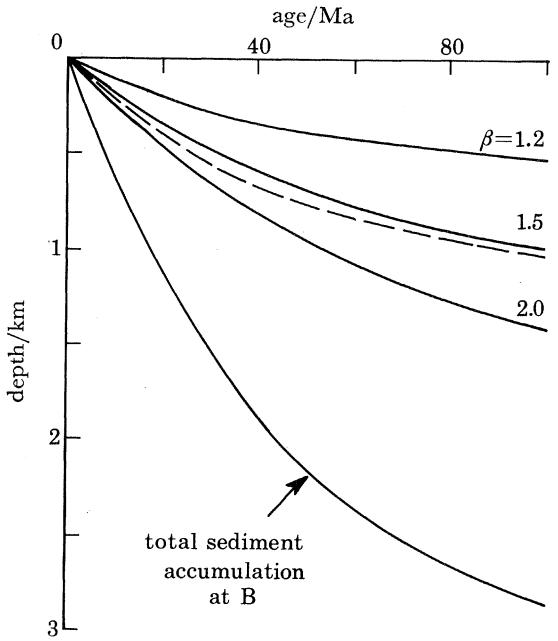

FIGURE 17. Sediment accumulation through time at B in the centre of the sedimentary basin in figure 13*c*. The solid lines indicate the subsidence that would have occurred at B if sediments had not infilled the basin. The broken line is the subsidence at B that would have been inferred from the sediments if they had been 'backstripped' by using an Airy rather than a flexure model. The best fit to the 'backstripped' curve is for $\beta = 1.6$ which is about a 40% smaller extension factor than actually assumed at B ($\beta = 2.0$).

(*c*) *Sea level changes through geological time*

The main problem in determining sea level changes through geological time is in separating tectonic from eustatic effects (see, for example, Fairbridge 1961). Relatively long-term changes of sea level have been estimated, based on changes in the volume of mid-ocean ridges through time (Hays & Pitman 1973; Pitman 1978), percentage estimates of continental flooding (Wise 1974), and tectonic processes in continental interiors (Bond 1978) and margins (Watts & Steckler 1979). These studies are in general agreement that there was a rise of sea level from the late Jurassic to the early Cretaceous and a relative fall since the late Cretaceous, although they differ in size by as much as a factor of 2 to 3. Vail *et al.* (1977) have suggested, based on the recognition of sedimentary sequences on seismic reflexion profiles, that superimposed on these long-term changes are a number of short-term fluctuations. They recognized slow rises in sea level followed by abrupt falls. The major periods of sea level rise were grouped by Vail *et al.* (1977) into supercycles, varying in age from about 5 Ma in the Tertiary to about 100 Ma in the Palaeozoic.

There is considerable debate at present about whether the supercycles identified by Vail *et al.* (1977) represent eustatic changes in sea level or widespread tectonic events. As Donovan & Jones (1979) have pointed out, the supercycles inferred by Vail *et al.* (1977) are based on seismic reflexion and well data that are largely unpublished. It is therefore difficult to determine whether

Vail *et al.* (1977) have taken into account those other factors that affect the stratigraphic record, such as compaction, palaeobathymetry and tectonic subsidence (Watts & Steckler 1979). Bally (1980) has argued, in fact, that many of the unconformities separating the cycles of Vail *et al.* (1977) may be due to major plate tectonic reorganizations rather than eustatic sea level changes.

The principal method by which Vail *et al.* 1977) and Vail & Todd (1982) estimate sea level rise in the stratigraphic record is by recognition of coastal onlap. They use seismic reflexion profiles at the edges of sedimentary basins, in conjunction with lithological and palaeontological data from nearby wells and seismic facies analysis, to estimate the vertical component of coastal onlap (coastal aggradation) for different geological time intervals. They then use a weighted average of coastal onlap estimates from various basins to infer eustatic sea level rise.

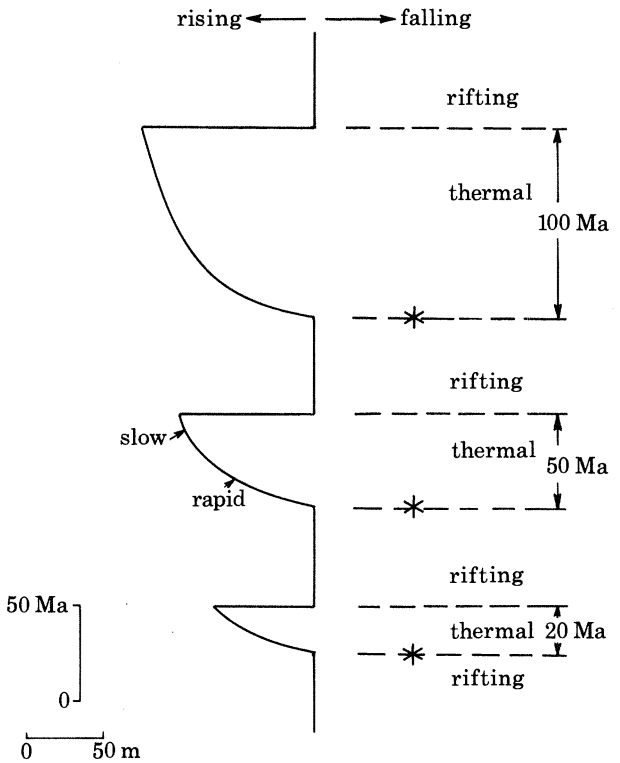

FIGURE 18. 'Apparent' sea-level changes inferred from the stratigraphy at the edge of the basin in figure 13*c*, by assuming that the progressive onlap of sediments at the edge of the basin represents a sea level rise. The changes have been calculated for assumed 20, 50 and 100 Ma durations of thermal subsidence in the basin.

We have shown in this paper that coastal onlap of the type used by Vail *et al.* (1977) and Vail & Todd (1982) to estimate sea level rise can be produced by sedimentary loading of a lithosphere that increases its flexural strength with time. For example, figure 18 shows the 'apparent' sea level rise that would be predicted from the stratigraphy at the edge of the basin in figure 13*c*, for different times after its initiation. The sea level rise is initially rapid and then slows, due to the increase of T_e with age. There is a striking resemblance between the overall shape of the apparent sea level rise and the shape of the sea level rise inferred by Vail *et al.* (1977) from the stratigraphic record.

This study suggests that some of the cycles identified by Vail *et al.* (1977) as due to a sea level rise may in fact have a tectonic rather than a eustatic control. Figure 19 compares the relative

changes of sea level inferred by Vail *et al.* (1977) since the Triassic with major tectonic events associated with the break-up of the Pangaea supercontinent. There is a good correlation between the unconformities separating the supercycles with the age of the rift–drift transition recorded in the stratigraphy of continental margins formed as a result of break-up. The rift–drift transition

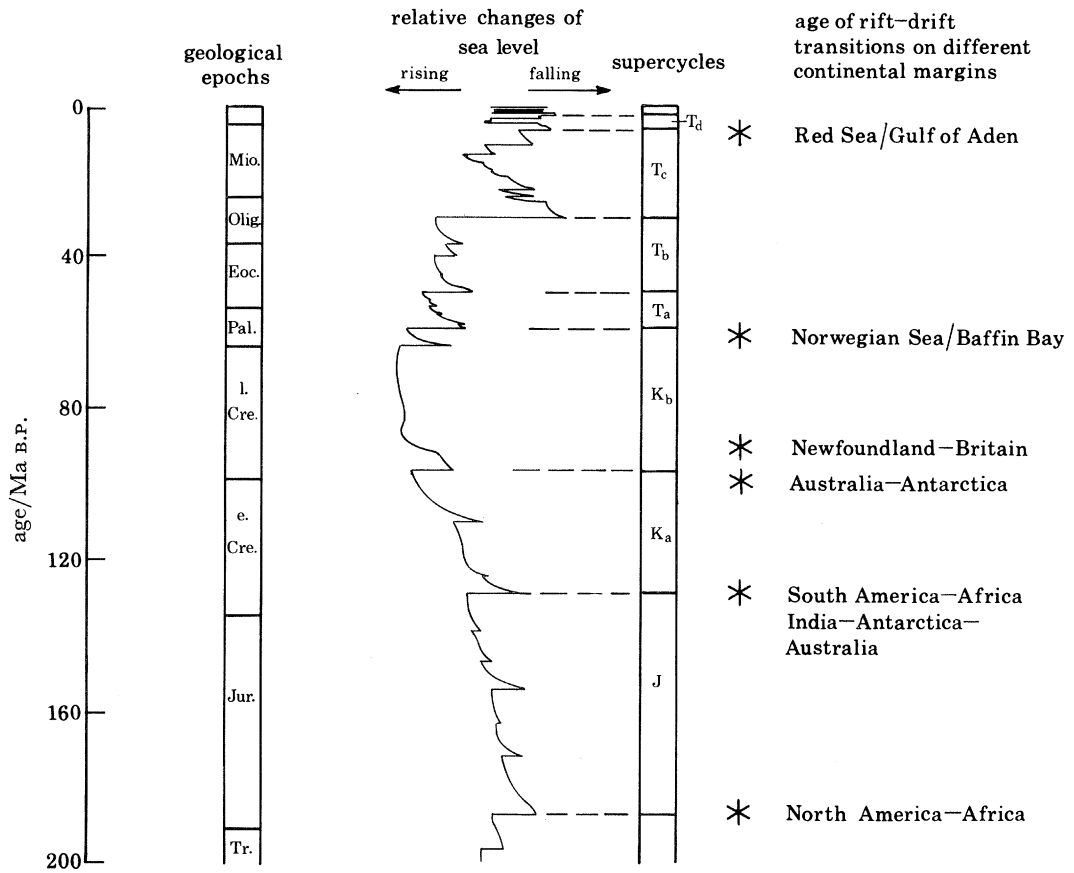

FIGURE 19. 'Relative changes in sea-level' based on Vail *et al.* (1977). A similar curve has recently been referred to by Vail & Todd (1982) as 'relative changes in coastal onlap'. Their preferred new Jurassic and early Cretaceous sea level curve, however, closely approximates that of Vail *et al.* (1977). The asterisks represent the approximate time of the rift-drift transition recorded in continental margins formed by the break-up of Pangaea. There is a good correlation between the beginning of some of the major supercycles of Vail *et al.* (1977) and major tectonic events in the ocean basins. The main exception is the beginning of supercycle T_c which, as pointed out by Vail *et al.* (1977), cannot in fact be correlated worldwide.

corresponds at most margins to the age separating fault-controlled from flexural-controlled subsidence. Thus, each margin after rifting would be expected to show coastal onlap as the lithosphere cools and increases its flexural strength with age. The supercycles identified by Vail *et al.* (1977) may therefore be widespread because the age of the rift–drift transition is similar for a number of widely separated margins (figure 19). We suggest, however, that the supercycles are not necessarily worldwide.

These considerations suggest that in order to estimate short-term variations in sea level it is necessary to consider sedimentary sequences that are not dominated by flexure, such as sediments associated with the rifting phase of continental margin basins or the oscillatory phase of interior and cratonic basins. The separation of eustatic and tectonic effects, however, will require detailed

studies of the subsidence and uplift history of widely separated sedimentary basins in continental margin, interior, and cratonic basins. The data required for these studies include multichannel seismic reflexion profiles and down-hole geological and geophysical well logs. Unfortunately, many of these data are not widely available at present.

6. Conclusions

We conclude the following from this study of lithospheric flexure and the evolution of sedimentary basins.

1. The dominant mechanisms affecting basin subsidence are thermal contraction following heating and thinning of the lithosphere at the time of their formation, and sedimentary loading. Thermal contraction controls the overall shape of basin that is available for sedimentation, whereas sedimentary loading is the main control on the stratigraphy of a basin.

2. The best fit to the overall basin geometry and stratigraphy is for an elastic plate model in which the flexural strength increases with time after basin initiation as the lithosphere cools.

3. The elastic plate model predicts a number of tectonic–stratigraphic features of basins including the increase in their overall width during evolution (West Siberia, Gippsland, North Sea during the Permian, coastal plains of Atlantic-type continental margins) and the progressive onlap of younger sediments onto basement at the basin edges.

4. The elastic plate model can also explain basins in which the youngest sediments are restricted to the basin centre (Michigan, Paris, Gulf coastal plain) if the sedimentary, or flexural controlled, cycle is followed by erosion of the basin or its edges, or both.

5. The elastic plate model is consistent with observations of flexure in the region of other geological loads on the lithosphere such as seamounts and oceanic islands, ice sheets, and an oceanic or continental plate as it approaches a deep-sea trench. In the oceans the flexural flexural strength of the lithosphere increases with age away from a mid-ocean ridge crest, while in the continents, the flexural strength appears to increase with age after a thermal event.

6. The role of flexure varies as a function of both time and position during the evolution of a basin and is an important factor to consider in 'backstripping' sedimentary loads through geological time. The use of an Airy model rather than a flexure model may, for example, lead to a significant underestimate of the amount of extension across a basin.

7. The elastic plate model predicts coastal onlap at the edges of basins of a type similar to that used by Vail *et al.* (1977) to infer relative rise in sea level through geological time. Thus many of the supercycles identified by Vail *et al.* (1977) may have a flexural (or tectonic) rather than a eustatic control.

8. The boundaries of most of the supercycles of Vail *et al.* (1977) appear to correlate with major tectonic events associated with the break-up of Pangaea. Thus the supercycles identified by Vail *et al.* (1977) may be widespread because a number of widely separated continental margins are characterized by similar ages for the transition from fault-controlled to flexural-controlled subsidence, but they are unlikely to be world wide.

We thank Jim Cochran, Dan McKenzie, F.R.S., and an anonymous reviewer for their helpful comments on the manuscript. Major support for this work was provided by National Science Foundation grants numbers OCE 79-18917 and OCE 79-26308. Additional support was provided by an Australian Public Service Post-Graduate Scholarship to G.D.K. and a Phillips Petroleum Fellowship to M.S.S.

PHILOSOPHICAL TRANSACTIONS OF THE ROYAL SOCIETY A MATHEMATICAL, PHYSICAL & ENGINEERING SCIENCES

Appendix. Two-dimensional stretching model

In order to model accurately the subsidence and sediment accumulation in sedimentary basins, it is necessary to include horizontal as well as vertical conduction of heat in model calculations. Variations in extension across basins can produce large horizontal thermal gradients and substantial lateral heat flow, altering the temperature distribution and therefore the elastic thickness T_e.

The appropriate equation to solve is the two-dimensional heat-flow equation,

$$\frac{\partial^2 T}{\partial x^2}+\frac{\partial^2 T}{\partial z^2}=\frac{1}{\kappa}\frac{\partial T}{\partial t}, \tag{A 1}$$

where $T = T(x, z, t)$ is the temperature distribution within the lithosphere, x is distance, z is depth (positive downwards), t is time, and k is the thermal diffusivity of the lithosphere. In general, the initial vertical temperature distribution will vary as a function of x as well as z and therefore an analytic solution cannot be guaranteed. If, however, the lithosphere is divided into a series of vertical blocks with a uniform initial vertical temperature distribution within each block and varying independently from block to block, then $T(x, z, t)$ can be expressed as a product of solutions of simpler differential equations than (A 1).

Following Carslaw & Jaeger (1959, p. 33), the temperature distribution in the lithosphere due to the thermal perturbation in one block is

$$T(x, z, t) = X(x, t)\, Z(z, t) \tag{A 2}$$

where
$$\frac{\partial^2 X}{\partial x^2}=\frac{1}{\kappa}\frac{\partial X}{\partial t} \quad \text{and} \quad \frac{\partial^2 Z}{\partial z^2}=\frac{1}{\kappa}\frac{\partial Z}{\partial t}. \tag{A 3}$$

Taking the z coordinate first, we have the one-dimensional heat-flow equation, the solution of which is the simple stretching model (McKenzie 1978)

$$Z(z,t) = T_0\frac{z}{a}+\sum_{n=1}^{\infty}\frac{2}{n\pi}\left\{\frac{\beta}{n\pi}\sin\left(\frac{n\pi}{\beta}\right)\right\}\sin\left(\frac{n\pi z}{a}\right)\mathrm{e}^{-n^2\pi^2\kappa t/a^2}. \tag{A 4}$$

Equation (A 4) consists of two parts, a steady-state temperature gradient and a thermal transient due to the instantaneous stretching, $\zeta(z, t)$, which has the form

$$\zeta(z, t) = \sum_{n=1}^{\infty}\frac{2}{n\pi}\left\{\frac{\beta}{n\pi}\sin\left(\frac{n\pi}{\beta}\right)\right\}\sin\left(\frac{n\pi z}{a}\right)\mathrm{e}^{-n^2\pi^2\kappa t/a^2}. \tag{A 5}$$

In the x direction, the boundary conditions on each block are such that the lithosphere is continuous and the solution becomes (Carslaw & Jaeger 1959)

$$X(x, t) = \tfrac{1}{2}(\pi\kappa t)^{-\frac{1}{2}}\int_{-\infty}^{\infty} X(x', 0)\,\mathrm{e}^{-(x-x')^2/4\kappa t}\,\mathrm{d}x'. \tag{A 6}$$

The initial conditions, $X(x', 0)$, corresponding to a single block, is $X = 1$ between a and b, the limits of the block, and $X = 0$ otherwise. This gives the result

$$X(x, t) = \frac{1}{2}\left[\mathrm{erfc}\left\{\frac{x-a}{(4\kappa t)^{\frac{1}{2}}}\right\}-\mathrm{erfc}\left\{\frac{x-b}{(4\kappa t)^{\frac{1}{2}}}\right\}\right]. \tag{A 7}$$

PHILOSOPHICAL TRANSACTIONS OF THE ROYAL SOCIETY A MATHEMATICAL, PHYSICAL & ENGINEERING SCIENCES

The full solution for the temperature distribution in the lithosphere is therefore

$$T(x,z,t) = T_0\frac{z}{a}+\frac{1}{2}\left[\operatorname{erfc}\left(\frac{x-a}{(4\kappa t)^{\frac{1}{2}}}\right)-\operatorname{erfc}\left(\frac{x-b}{(4\kappa t)^{\frac{1}{2}}}\right)\right]\zeta(z,t), \tag{A 8}$$

where it is assumed that the steady-state temperature gradient is the same for the entire lithosphere. The temperature structure due to the stretching of a single block is essentially the same as (A 4), but now the transient solution spreads laterally according to the error function distribution.

Since the heat-flow equation is linear, the law of superposition can be applied to give the temporal temperature structure of lithosphere containing a number of stretched blocks. The temperature in any block is then a weighted sum of the one-dimensional solution of the temperature field of that block and all the surrounding blocks where the weighting is given by the error function

$$T(x,z,t) = T_0\frac{z}{a}+\sum_{i=1}^{n_{\mathrm{box}}}\frac{1}{2}\left[\operatorname{erfc}\left(\frac{x-x_i}{(4\kappa t)^{\frac{1}{2}}}\right)-\operatorname{erfc}\left(\frac{x-x_{i+1}}{(4\kappa t)^{\frac{1}{2}}}\right)\right]\zeta_i(z,t), \tag{A 9}$$

where x_i and x_{i+1} are the position of edges of block i, $\zeta_i(z,t)$ is the transient temperature solution for that block, and n_{box} is the number of stretched blocks.

The thermal expansion can be calculated from the vertical integral of (A 9). Thus the thermal expansion can be computed in a similar way to the temperature structure as the solution for the one-dimensional equation diffusing laterally according to an error function.

Bibliography (Watts *et al.*)

Artemjev, M. & Artyushkov, E. V. 1971 *J. geophys Res.* **76**, 1197–1971.

Bally, A. W. 1980 In *Dynamics of plate interiors* (*Geodynamics series*, vol. 1) (ed. A. W. Bally, P. L. Bender, T. R. McGretchin & R. I. Walcott), pp. 5–10.

Bally, A. W. & Snelson, S. 1980 In *Facts and principles of world petroleum occurrence* (*Can. Soc. Petrol. Geol. Mem. no.* 6) (ed. A. Mull), pp. 9–94.

Banks, R. J., Parker, R. L. & Huestis, S. P. 1977 *Geophys. Jl R. astr. Soc.* **51**, 431–542.

Barrell, J. 1914 *J. Geol.* **22**, 425–443.

Beaumont, C. 1978 *Geophys. Jl R. astr. Soc.* **55**, 471–498.

Beaumont, C. 1981 *Geophys. Jl R. astr. Soc.* **65**, 291–329.

Beaumont, C. & Sweeney, J. F. 1978 *Tectonophysics* **50**, T19–23.

Bodine, J. H. 1981 *Lamont-Doherty Geol. Obs., tech. Rep. no.* 1, CU-1-80 (36 pages).

Bodine, J. H., Steckler, M. S. & Watts, A. B. 1981 *J. geophys Res.* **86**, 3695–3707.

Bond, G. 1978 *Geology* **6**, 247–250.

Bott, M. H. P. 1973 In *Implication of continental drift to the earth sciences* (ed. D. H. Tarling & S. K. Runcorn), vol. 2, pp. 675–683. London and New York: Academic Press.

Bott, M. H. P. & Watts, A. B. 1970 *Nature, Lond.* **225**, 265–268.

Bowie, W. 1922 *Bull. geol. Soc. Am.* **33**, 273–286.

Bureau de Recherches Géologique et Minières (B.R.G.M.) 1980 *Synthèse géologique du Bassin de Paris*, vol 2. (Atlas). *Mem. B.R.G.M.* no. 102.

Caldwell, J. G. 1979 Ph.D. thesis, Cornell University. (151 pages.)

Caldwell, J. G., Haxby, W. F., Karig, D. E. & Turcotte, D. L. 1976 *Earth planet Sci. Lett.* **31**, 239–246.

Carslaw, H. S. & Jaeger, J. C. 1959 *Conduction of heat in solids.* (510 pages.) Oxford University Press.

Cazenave, A., Lago, B., Dominti, K. & Lambeck, K. 1980 *Geophys. Jl R. astr. Soc.* **63**, 233–254.

Christie, P. A. F. & Sclater, J. G. 1980 *Nature, Lond.* **283**, 729–732.

Cochran, J. R. 1973 *Bull. geol. Soc. Am.* **84**, 3244–3268.

Cochran, J. R. 1979 *J. geophys. Res.* **84**, 4713–4729.

Cohen, T. J. & Meyer, R. P. 1976 *Geophys. Monogr.* no. 19, pp. 431–438. Washington, DC.: American Geophysical Union.

Colquhoun, D. J. & Johnson, M. S. 1968 *Palaeogeog. Palaeoclimat. Palaeoecol.* **5**, 105–126.

Cravatte, J., Dufaure, P., Prim, M. & Rouaix, S. 1974 *Compagnie fr. Pétrol. Notes Mém.* **11**, 209–274.

Crittenden, M. D., Jr. 1967 *Geophys. Jl R. astr. Soc.* **14**, 261–279.

Crittenden, M. D., Jr 1970 *Can. J. Earth Sci.* **7**, 727–729.

PHILOSOPHICAL TRANSACTIONS OF THE ROYAL SOCIETY A MATHEMATICAL, PHYSICAL & ENGINEERING SCIENCES

Collette, B. J. 1960 *The gravity field of the North Sea, Gravity Expeditions, 1948–1958*, vol. 5, pt 2. Delft: Netherlands Geodetic Commission.
de Charpal, O., Guennoc, P., Montadert, L. & Roberts, D. G. 1978 *Nature, Lond.* **275**, 706–711.
Detrick, R. S. & Watts, A. B. 1979 *J. geophys. Res.* **84**, 3637–3653.
Dickinson, W. R. & Yarborough, N. 1976 In *Plate tectonics and hydrocarbon accumulation* (*Am. Ass. Petrol. Geol., Short Course, New Orleans*), pp. 1–56.
Donovan, D. & Jones, E. J. W. 1979 *J. geol. Soc. Lond.* **136**, 187-192.
Effimof, I. & Pinezich, A. R. 1981 *Phil. Trans. R. Soc. Lond.* A **300**, 435–442.
Fairbridge, R. W. 1961 In *Physics and chemistry of the Earth* (ed. L. N. Ahrens, F. Press, K. Rankama & S. K. Runcorn), pp. 99–115. London: Pergamon Press.
Falvey, D. A. 1974 *J. Aust. Petrol. Explor. Ass.* **14**, 95–106.
Fulton, R. J. & Walcott, R. I. 1975 *Mem. geol. Soc. Am.* no. 142, 163–173.
Goetze, C. & Evans, B. 1979 *Geophys. Jl R. astr. Soc.* **59**, 463–478.
Grow, J. A., Mattrick, E. R. & Schlee, J. S. 1979 In *Geological investigations of continental margins* (*A.A.P.G. Mem.* no. 29) (ed. J. S. Watkins, L. Montadert & P. W. Dickerson), pp. 65–83.
Hanks, T. 1971 *Geophys. Jl R. astr. Soc.* **23**, 173–189.
Haxby, W. F., Turcotte, D. L. & Bird, J. M. 1976 *Tectonophysics* **36**, 57–75.
Hays, J. & Pitman, W. C. 1973 *Nature, Lond.* **246**, 18–22.
Heiskanen, W. A. & Vening Meinesz, F. A. 1958 *The Earth and its gravity field.* (470 pages.) New York: McGraw-Hill.
Hocking, J. B., 1976 In *Geology of Victoria* (ed. J. G. Douglas & J. A. Ferguson) (*Geol. Soc. Aust. spec. Publ.* no. 5).
Holtedahl, H. & Bjerkji, K. 1975 *Norg. geol. Unders.* **316**, 241–252.
Jarrard, R. D. & Turner, D. L. 1979 *J. geophys. Res.* **84**, 5691–5694.
Karner, G. D. 1981 *Eos, Wash.* **62**, 390.
Karner, G. D. & Watts, A. B. 1982 *J. geophys. Res.* (In the press.)
Keen, C. E. 1979 *Can. J. Earth Sci.* **16**, 505–522.
Kent, P. 1976 *Tectonophysics*, **36**, 87–92.
Klemme, H. D. 1975 In *Petroleum and global rectonics* (ed. A. G. Fisher & S. Judson), pp. 251–305. Princeton University Press.
Kumar, N. 1978 *Bull. Am. Ass. Petrol. Geol.* **62**, 273–294.
Lawson, A. C. 1938 *Bull. geol. Soc. Am.* **49**, 401–416.
Le Pichon, X. & Sibuet, J.-C. 1981 *J. Geophys. Res.* **86**, 3708–3720.
Loncarevic, B. C. & Ewing, G. N. 1967 *Geophysical study of the Orpheus Gravity anomaly* (*Proc. 7th World Petrol. Cong.*). (828 pages.)
McAdoo, D. C., Caldwell, J. G. & Turcotte, D. L. 1978 *Geophys. Jl R. astr. Soc.* **54**, 11–26.
McConnell, R. K., Jr 1968 *J. geophys. Res.* **73**, 7089–7105.
McGinnis, 1970 *J. geophys. Res.* **75**, 317–331.
McKenzie, D. P. 1978 *Earth planet. Sci. Lett.* **40**, 25–32.
McKenzie, D. P. & Bowin, C. 1976 *J. geophys Res.* **81**, 1903–1915.
McNutt, M. K. 1979 *J. geophys. Res.* **84**, 7589–7598.
McNutt, M. K. & Menard, M. W. 1978 *J. geophys. Res.* **83**, 1206–1212.
McNutt, M. K. & Parker, R. L. 1978 *Science, Wash.* **199**, 773–775.
Molnar, P. & Tapponnier, P. 1980 *Earth planet. Sci. Lett.* **52**, 107–114.
Middleton, M. F. 1980 *Geophys. Jl R. astr. Soc.* **62**, 1–14.
Parsons, B. & Sclater, J. G. 1977 *J. geophys. Res.* **83**, 803–827.
Peltier, W. R. 1980 In *Dynamics of plate interiors* (*Geodynamics Series*, vol. 1) (ed. A. W. Bally, P. L. Bender, R. McGetchin & R. I. Walcott), pp. 111–129.
Pitman, W. C., III 1978 *Bull. geol. Soc. Am.* **89**, 1389–1406.
Profett, J. M., Jr. 1977 *Bull. geol. Soc. Am.* **88**, 247–266.
Royden, L. & Keen, C. E. 1980 *Earth planet. Sci. Lett.* **51**, 343–361.
Royden, L., Sclater, J. G. & von Herzen, R. P. 1980 *Bull. Am. Ass. Petrol. Geol.* **64**, 173–187.
Sclater, J. G. & Christie, P. A. 1980 *J. geophys. Res.* **85**, 3711–3739.
Sclater, J. G., Royden, L., Horváth, F., Burchfiel, B. C., Semken, S. & Stegena, L. 1981*a* *Earth planet. Sci. Lett.* **51**, 139–162.
Sclater, J. G., Parsons, B. & Jaupart, C. 1981*b* (In the press.)
Sleep, N. H. 1971 *Geophys. Jl R. astr. Soc.* **24**, 325–350.
Sleep, N. H., Nunn, J. A. & Chou, L. 1980 *A. Rev. Earth planet. Sci.* **8**, 624–000.
Sleep, N. H. & Snell, N. S. 1976 *Geophys. Jl R. astr. Soc.* **45**, 125–154.
Sleep, N. H. & Sloss, L. L. 1978 *J. geophys. Res.* **83** (B12), 5815–5819.
Sloss, L. L. & Scherer, W. 1975 *Mem. geol. Soc. Am.* no. 142, 71–88.
Sloss, L. L. & Speed, N. H. 1974 In *Tectonics and sedimentation* (ed. W. R. Dickinson), pp. 98–119.
Steckler, M. S. & Watts, A. B. 1978 *Earth planet. Sci. Lett.* **41**, 1–13.
Steckler, M. S. & Watts, A. B. 1980 *Nature, Lond.* **287**, 425–529.

PHILOSOPHICAL TRANSACTIONS OF THE ROYAL SOCIETY A MATHEMATICAL, PHYSICAL & ENGINEERING SCIENCES

Suyenaga, W. 1977 Ph.D. thesis, University of Hawaii. (147 pages.)
Sweeney, J. 1976 *Tectonophysics* **36**, 181–196.
Tanner, J. J. 1966 *J. Aust. Petrol. Explor. Ass.* **6**, 116–120.
Turcotte, D. L., Ahern, J. L. & Bird, J. M. 1977 *Tectonophysics* **42**, 1–28.
Vail, P. R., Mitchum, R. M. & Thompson, S. 1977 *Mem. Am. Ass. Petrol. Geol.* no. 26, pp. 83–97
Vail, P. R. & Todd, R. G. 1982 In *Proc. Conference on Petroleum Geology of the Continental Shelf of Northwest Europe*. (In the press.)
Walcott, R. I. 1970*a* *Can. J. Earth. Sci.* **7**, 716–727.
Walcott, R. I. 1970*b* *Can. J. Earth Sci.* **7**, 931–937.
Walcott, R. I. 1970*c* *J. geophys. Res.* **75**, 3941–3954.
Walcott, R. I. 1972 *Bull. geol. Soc. Am.* **83**, 1845–1848.
Walcott, R. I. 1976 In *International Woollard Symposium* (*A.G.U. Monograph* no. 19), pp. 431–438. Washington, D.C.: American Geophysical Union.
Watts, A. B. 1978 *J. geophys. Res.* **83**, 5989–6004.
Watts, A. B. 1981 Am. Ass. Petrol. Geol., Short Course, Atlantic City, New Jersey.
Watts, A. B. Bodine, H. J. & Ribe, N. M. 1980 *Nature, Lond.* **283**, 532–537.
Watts, A. B. & Cochran, J. R. 1974 *Geophys. Jl R. astr. Soc.* **38**, 119–141.
Watts, A. B., Cochran, J. R. & Selzer, G. 1975 *J. geophys. Res.* **80**, 1391–1398.
Watts, A. B. & Ryan, W. B. F. 1976 *Tectonophysics* **36**, 25–44.
Watts, A. B. & Steckler, M. S. 1979 In *Maurice Ewing Symposium Series*, vol. 3, pp. 218–234. Washington, D.C.: American Geophysical Union.
Watts, A. B. & Steckler, M. S. 1981 *Oceanological Acta* (*Proc. of 26th Int. Cong., Paris*), **4**, 143–153.
Watts, A. B. & Talwani, M. 1974 *Geophys. Jl R. astr. Soc.* **36**, 57–90.
Weaver, P. 1951 *Bull. Am. Ass. Petrol. Geol.* **35**, 393–398.
Wellman, P. 1979 *B.M.R. Jl Aust. Geol. Geophys.* **4**, 373–382.
Wendt, I., Kreuzer, H., Muller, P., Von Rad, U. & Raschka, 1976 *Deep Sea Res.* **23**, 849–862.
Winnock, E., 1971 In *Histoire structurale du Golfe de Gascogne*, vol. 1 (*Collection collogues et seminaires*), p. 22. Institut Français du Pétrole, 1-1-1-30.
Wise, D. U. 1974 In *The geology of continental margins* (ed. C. A. Burke & C. L. Drake), pp. 45–58.
Wood, R. J. 1981 *Earth planet. Sci. Lett.* **54**, 306–312.
Zhabrev, I. P., Zubov, I. P., Krylov, N. A. & Semenovich, V. V. 1975 In *Proceedings of the Ninth World Petroleum Congress*, vol. 2 (Geology), pp. 83–91.
Ziegler, P. A. 1977 *Geol. J.* **1**(1), 7–32.
Ziegler, P. A. 1978 *Geologie Mijnb.* **57**, 589–626.
Ziegler, P. A. & Louwerens, C. J. 1977 *Acta Univ. Ups. Symp.*, vol. 2, pp. 7–22.

PHILOSOPHICAL TRANSACTIONS OF THE ROYAL SOCIETY A MATHEMATICAL, PHYSICAL & ENGINEERING SCIENCES